USDA Agricultural Research Service
U.S. DEPARTMENT OF AGRICULTURE

Evaluation of Drywell Performance at Fort Irwin

Final Report 2021

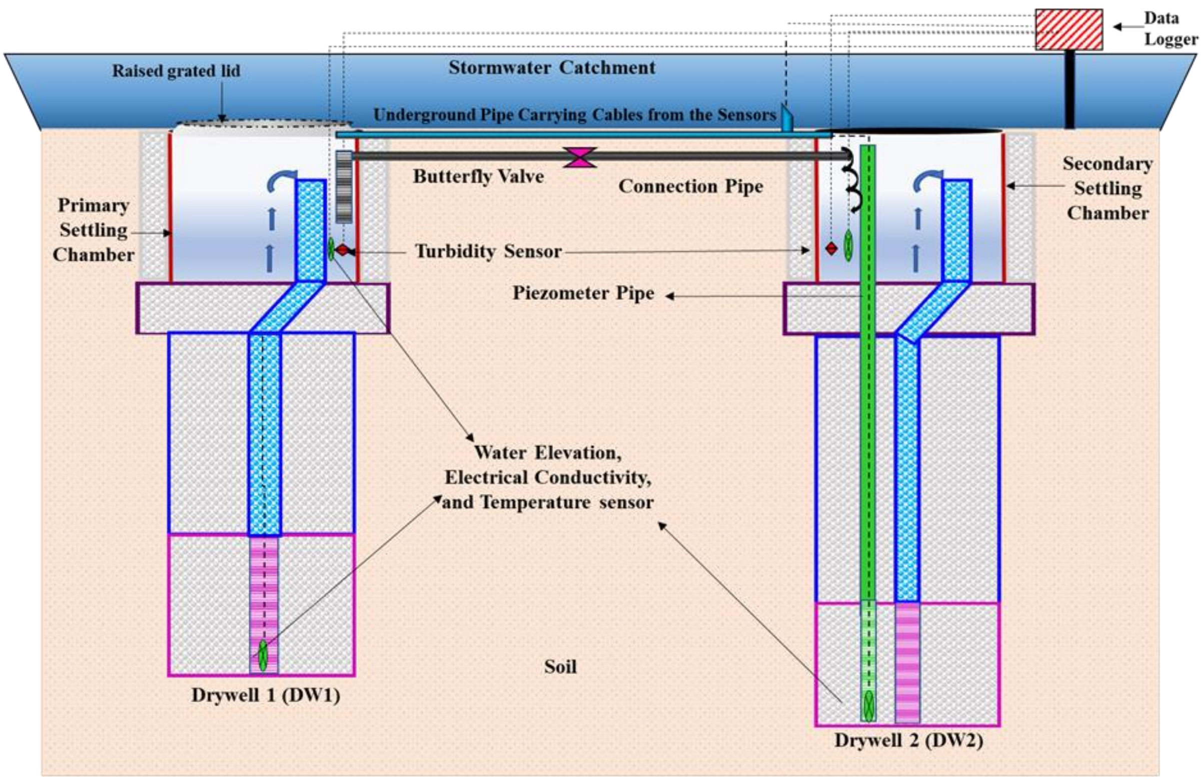

Research Support for Watershed and Basin Hydrology and Water Quality in the Arid and Semi-Arid Southwest, USDA

In partnership with: USDA | UC Riverside | EPA

Published February 18, 2022

RESEARCH SUPPORT FOR WATERSHED AND BASIN HYDROLOGY AND WATER QUALITY IN THE ARID AND SEMI-ARID SOUTHWEST, USA

Evaluation of Drywell Performance at Fort Irwin: Vadose Zone Study Final Report 2021

Salini Sasidharan [1, 2], Scott A. Bradford[2, 3], Jirka Šimůnek[1]

[1] Department of Environmental Sciences, University of California, Riverside, CA 92521, USA

[2] United States Department of Agriculture, Agricultural Research Service, Salinity Lab, Riverside, CA 92507, USA

[3] United States Department of Agriculture, Agricultural Research Service, Sustainable Agricultural Water Systems Unit, Davis, CA 95616, USA

DOCUMENT CONTROL SUMMARY

Title:	Research Support for Watershed and Basin Hydrology and Water Quality in the Arid and Semi-arid Southwest, USA
Subtitle:	Evaluation of Drywell Performance at Fort Irwin: Vadose Zone Study Final Report 2021
Client Company:	US Environmental Protection Agency
Client Contact:	Steve Kraemer
Status:	Final
Project Manager	Scott A. Bradford
Author(s):	Salini Sasidharan, Scott A Bradford, Jirka Simunek
Revision Number:	Final
EPA Interagency Agreement No.	DW-012-92465401-5
Date:	10/15/2021
Checked By:	Scott A. Bradford
Issued By:	Salini Sasidharan

PERSONNEL

Dr. Salini Sasidharan

Postdoctoral Scientist

Department of Environmental Sciences,

University of California, Riverside,

CA 92521, USA

Email: salinis@ucr.edu, Salini.Sasidharan@oregonstate.edu

Dr. Scott A. Bradford

Research Leader

USDA, ARS, Sustainable Agricultural Water Systems (SAWS) Unit

239 Hopkins Road

UC Davis, Davis, CA 95616

Email: Scott.Bradford@usda.gov

Prof. Jirka Šimůnek

Professor of Hydrology & Hydrologist

Department of Environmental Sciences,

University of California, Riverside,

CA 92521, USA

Email: Jiri.Simunek@ucr.edu

Preferred Citation for the Document for Chapter 1 and Chapter 7: Sasidharan, S., Bradford, S.A., and Simunek, J., (2021), Evaluation of Drywell Performance at Fort Irwin: Vadose Zone Study Final Report 2021, Research Support for Watershed and Basin Hydrology and Water Quality in the Arid and Semi-arid Southwest, USA, US Environmental Protection Agency, pp. 1-66

TABLE OF CONTENT

ABSTRACT

Groundwater is a significant source of drinking water in urban and rural regions of the southwest United States. However, the continuous demand induces unsustainable withdrawal of groundwater resources, which are limited by natural or artificial recharge. Concurrently, significant flood events are a reoccurring problem in California that causes billions of dollars worth of infrastructure damage. Therefore, new engineering solutions must be developed, tested, and implemented to mitigate flooding, enhance groundwater recharge, and ensure drink water quality. Managed aquifer recharge (MAR) is a cross-cutting technology expanding in popularity and intensity to improve groundwater resources. MAR can be accomplished through a variety of approaches such as infiltration basins, flooding agricultural land, and vadose zone recharge wells like drywells. Urban and rural flooding, groundwater recharge, and freshwater supplies in arid and semiarid areas can be significantly improved by successfully implementing low-impact green infrastructures. Drywells are widely used as a best management practice in urban areas for stormwater management. We have explored the potential use of drywells as a MAR technique for flood mitigation and groundwater recharge at an Army basin in Mojave desert of California, USA. This project supports the long-term goals of the Army's Net Zero Water program. Despite the popularity of drywells at commercial sites, the impact of drywells on groundwater resources from both a quantitative and qualitative perspective has previously not received much scientific study.

This report document results from a four-year drywell study (2017-2021) in Fort Irwin, CA. A newly installed drywell was connected to a pre-existing drywell using connections pipes. Several water level and turbidity measuring sensors were installed in the drywells, and data were continuously collected. A monitoring well was installed with several vadose zone monitoring sensors (water content sensor, perched water table level sensor, and groundwater level sensor). The site hydraulic conductivity was determined using falling head tests, soil characterization, and numerical modeling. The 4-year monitoring study demonstrated that the new drywell mitigated the ponding problem at the site and drained the catchments within a few days after a storm event, compared to a few weeks before the project execution. The site geology investigation revealed an extensive clay layer below the drywell that inhibited direct recharge from the drywell over the monitoring zone. The clay layer resulted in the development of a perched water table at the site. Additional research was conducted to evaluate the performance of drywells, including to understand the effect of deterministic and stochastic subsurface heterogeneity on infiltration, recharge, and virus transport under constant head conditions. Additionally, research was conducted to compare the infiltration and recharge behavior from an infiltration basin with several drywells. The research outcomes were published as five peer-reviewed research manuscripts in high-impact journals (J. Hydrology, Advances in Water Resources, and Water Research). In addition, the research was presented in national and international conferences such as the ASA-SSSA-ASSA meeting and AGU meeting. The research has also attracted local agencies

such as Orange County Water District, California Water Board, and farmers across the state.

CHAPTER 1

Fort Irwin

Study Site and Research Objective

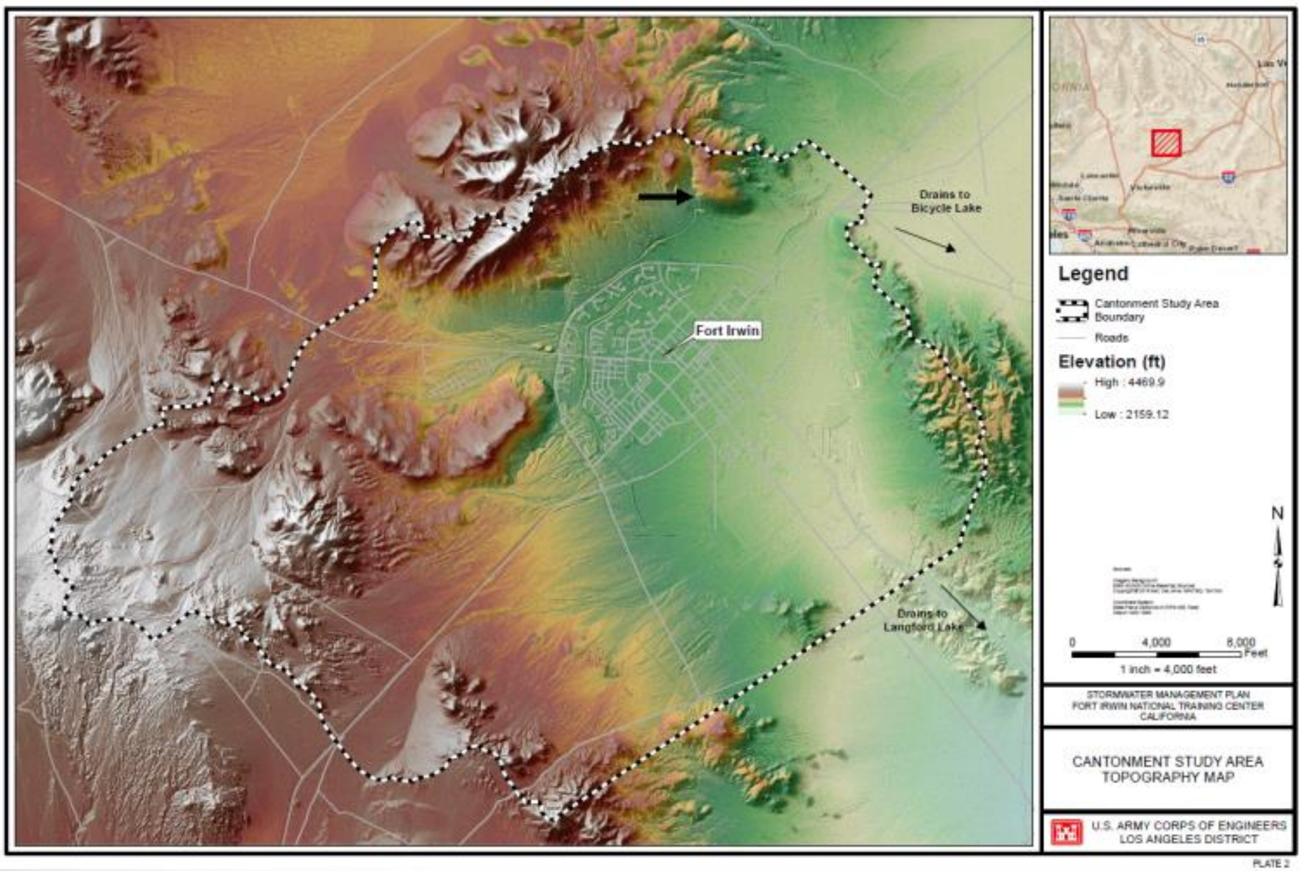

1. Changing Climate and Water Crisis

Severe and persistent 21st-century drought in southwestern North America is comparable to the medieval megadroughts. The hydrological modeling and new 1200-year tree-ring reconstructions of summer soil moisture to demonstrated that the 2000–2018 drought was the second driest 19-year period since 800 CE, exceeded only by a late-1500s megadrought. The megadrought-like trajectory of 2000–2018 soil moisture was driven by natural variability superimposed on drying due to anthropogenic warming (Williams et al., 2020). The 21st-century drought severity has been reflected in reduced snowpack (Mote et al., 2018), reduced river flow and lake levels (Xiao et al., 2018), declines in groundwater availability (Rodell et al., 2018), shifts in agricultural activities (Howitt et al., 2014), forest drought stress (Williams et al., 2013), increased wildfire activity (10), and reduced vegetation carbon uptake (Schwalm et al., 2012).

Groundwater is a major source for drinking water to urban and rural regions in the southwest US, which have had rapid growth of population, agriculture, and industry in the last few decades. Groundwater is a vital component of California's urban and rural water supply. On average, underground aquifers provide nearly 40% of the water used by California's farms and cities and significantly more in dry years. About 85% of Californians depend on groundwater for some portion of their water supply. Some communities rely entirely on groundwater for drinking water, and it is a critical resource for many farmers in the Central Valley and Central Coast (Chappelle et al., 2017). However, the continuous demand induces unsustainable withdrawal of groundwater resources, which are limited by natural or artificial recharge. The resulting overdraft and its repercussions can include higher energy use to pump water from deeper wells, land subsidence (which can damage vital infrastructures such as canals, levees, and roads), reduced streamflow, and reduced water quality (especially in coastal aquifers, which draw in seawater when depleted) (Faunt et al., 2016; Ghasemizade et al., 2019). The problem is worsened by the frequent severe drought conditions in arid and semiarid area. In contrast to surface water, groundwater use has largely been unregulated under California law until recently. In general, a primary goal of managing groundwater resources in these regions is to achieve long-term sustainable usage of water resources based mainly on water conservation and enhancement of groundwater recharge. The local and state governments, and policy- and decision-makers formed the Sustainable Groundwater Management Act (SGMA) in 2014, to manage groundwater extraction and protect groundwater resources for the future (Harter, 2015). SGMA recognizes that groundwater is best managed at the local level due to the variabilities in geographic, geologic, and hydrologic parameters and provides 20 years to implement reliable groundwater management plans to achieve long-term groundwater sustainability (Faunt et al., 2016).

Concurrently, significant flood events during early winter are a reoccurring problem in California. Rising global temperature can increase storm temperatures and atmospheric water-vapor transport rates, which will increase the frequency and severity of floods in California over the next 100 years (Dettinger, 2011; Kocis and Dahlke, 2017). In addition, greenhouse emissions from agricultural activities (Lal and Logan, 1995), rising global temperature (Kerr, 2001), sea-level rise (Heberger et al., 2011), floodplain urbanization (Montz, 2000), reductions in the snowpack, and shifts from snowfall to rainfall (Hanak and Lund, 2012) seem likely to increase flood peak flows and flood volumes. Floods are very costly natural disasters that can cause immense damage to human societies. For example, the total estimated flood damage in California for 2017 was almost $1.05 billion (Wamsley, 2017; Wright, 2019). In order to adapt to these extreme climate challenges, California is developing strategies to capture excess floodwater and recharge groundwater aquifers for reliable multi-year storage (Kocis and Dahlke, 2017). Successful implementation of this strategy provides an opportunity to mitigate both flood damage and groundwater depletion problems simultaneously.

Groundwater contamination is another growing water quality problem. In many rural areas, nitrate—produced by nitrogen fertilizer and manure—is polluting local drinking water supplies. In some urban areas, basins are contaminated by industrial chemicals or flame retardants. Salt accumulation in inland basins and saltwater intrusion in some coastal groundwater basins can damage crops and contaminate drinking water supplies. Microbial migration and contamination in drinking water wells and subsequent disease outbreaks are widespread in many parts of the world. Treatment to remove contaminants from drinking water is costly, especially for small rural systems. Efforts are underway to find near-term solutions for poor rural communities with unsafe drinking water and reduce future contamination of the state's aquifers by controlling industrial discharges and changing farming practices (Chappelle et al., 2017). In a state where water is already scarce, the contamination of wells adds another unwelcome stressor.

2. Managed Aquifer Recharge and Low Impact Development Techniques

Several tools or engineered solutions have been developed for better groundwater management across the world. California's groundwater basins can store large volumes of additional water—at least three times more than the state's existing dams. The SGMA provides local agencies the tools and authority they need to develop and implement plans that will bring their basins into balance. Achieving this goal will protect the state's groundwater reserves for the long term and enable its residents and economy to better handle future droughts. But attaining balance will require difficult decisions because water use and irrigated acreage may need to decline to close the groundwater deficit (Chappelle et al., 2017).

Managed aquifer recharge (MAR) is a cross-cutting technology (Sprenger et al., 2017) that has been expanding in popularity and intensity to improve groundwater resources (Ghasemizade et al., 2019). MAR is the intentional diversion, transport, storage, infiltration, and recharge of excess surface water (snowmelt, streamflow, and stormwater) into aquifers during a wet period for subsequent recovery during dry periods or environmental benefit (Dillon et al., 2010). MAR can be accomplished through a variety of approaches such as infiltration basins (Teatini et al., 2015), aquifer storage and recovery (Dillon et al., 1999), aquifer storage, transfer, and recovery (Pavelic et al., 2005), flooding land (Flood-MAR) (Scherberg et al., 2014), flooding agricultural land (Ag-MAR) (Niswonger et al., 2017), and vadose zone recharge wells like drywells (Sasidharan et al., 2018; Sasidharan et al., 2019; Sasidharan et al., 2020).

Water supplies in arid and semiarid areas can be significantly improved if developers and planners have verified modeling tools to predict the amount of stormwater generated from development and the amount of that water that can be effectively recharged into groundwater aquifers or used to offset groundwater pumping by using distributed, Low Impact Development (LID) and Green Infrastructure (GI) best management practices (BMPs). An increase in impervious surfaces such as buildings, roads, parking lots, and compacted soil reduces infiltration, causes localized flooding, and increases pollutants in surface runoff (Cantone and Schmidt, 2011). Urbanization has resulted in a nearly 26-fold increase in runoff over the natural watershed, and compaction of soils due to home lot, and subdivision construction accounted for roughly 15-20% of the total increase in runoff (Kennedy et al., 2013a; Kennedy et al., 2013b). Impervious surfaces contribute to the development of urban heat islands as a result of rapid water runoff, reductions in evapotranspiration, and drops in groundwater levels (Rizwan and Bhattacharjee, 2009). Past stormwater practices in humid and arid regions relied primarily on grey infrastructure (centralized, hardscape conveyances) to rapidly export stormwater to downstream areas while attempting to detain flows long enough to reduce peak runoff rates to predevelopment peak flows. Increased runoff typically results in lower groundwater recharge and base flows in humid regions.

However, increase in runoff volumes due to development in arid and semiarid environments results in "new" manageable water that would otherwise be evaporated or transpired by desert vegetation after infiltration into non-channelized areas. This "new" water provides an opportunity to augment the water supply by recharging stormwater or using it to promote greenness and create a more livable, healthier environment while offsetting groundwater pumping for landscape watering. Ideally, the "best" outcome to an integrated watershed plan would be to maintain peak flows and runoff volumes at the predevelopment levels, minimize pollutant loads, and capture stormwater to augment the water supply. It is essential to consider upstream land uses that can have an impact on runoff water quality. In addition to urbanization, military training, vegetation cover, and wildfires can substantially impact the quantity and quality of runoff.

Since traditional urban drainage systems, composed of a network of pipes, have proven to be inadequate in managing a constant increase of surface runoff, Low Impact Development (LIDs) or Water Sensitive Urban Design (WSUD) techniques (Kazemi et al., 2018) are gaining popularity among practitioners. These techniques mitigate adverse effects of urbanization by improving stormwater retention close to its source, removing contaminants from stormwater, and enhancing groundwater recharge and evapotranspiration. LID is a "green" approach that aims to maintain or replicate the predevelopment hydrological regime by using the Best Management Practices (BMP). BMPs are microscale and decentralized management techniques that include green roofs, permeable pavements, vegetated filter strip, bioretention systems, and infiltration systems such as drywells or infiltration trenches. BMPs can reduce surface runoff and associated contaminants by increasing infiltration and exploiting adsorption and filtration, respectively (U.S.EPA, 2021).

3. Challenges and Knowledge Gap

While the effectiveness of LIDs on surface runoff has been well documented and studied (Bengtsson et al., 2004; Carbone et al., 2014; Davis, 2008; Getter et al., 2007), the effects of LIDs on groundwater resources have been only partially investigated. Recharge beneath LIDs has been previously modeled or estimated as a percentage of precipitation. Some studies estimated that between 40 and 99% of rainfall became recharge beneath LIDs (Dietz and Clausen, 2006; Endreny and Collins, 2009; Stephens et al., 2012). In Arizona, recharge beneath LIDs has been estimated as a fraction of captured runoff that does not evaporate using the Curve Number method. Some municipalities have implemented groundwater recharge studies for large-scale and centralized MAR sites, often using yearly water budgets and field-calibrated groundwater flow models to predict recharge (Hanson et al., 2010; Racz et al., 2012). Findings from these prior studies indicate that recharge beneath LIDs is likely controlled in part by the precipitation intensity and duration, runoff characteristics of the impervious cover connected to the BMP, soil properties, including hydraulic conductivity, and the storage capacity of the BMP facility (Shuster et al., 2007).

Infiltration systems, such as infiltration trenches and basins, French drains, and drywells can significantly impact groundwater resources. A drywell is a subsurface storage facility that receives and temporarily stores stormwater runoff from rooftops and other impervious surfaces. They are deeper and less wide than infiltration trenches. Discharge of the stored runoff from a drywell occurs through infiltration into the surrounding soil. A drywell may be either a structural chamber and/or an excavated pit filled with aggregate. Drywells are usually equipped with an overflow system that ensures that additional runoff is safely and efficiently conveyed downstream. Modern drywell designs include systems of sedimentation chambers, deep casings, and chemical absorbing sponges, overflow pipe, gravel-filled lower chambers, geotextile membrane (MaxWell IV), and in some cases, a connection pipe with a primary and secondary chamber (Maxwell Plus) (Torrent Resources, http://www.torrentresources.com/). Drywells can be used to reduce an increased volume of stormwater runoff caused by roofs of buildings. Roofs are one of the most important sources of new or increased runoff volume from land development sites. As stated above, drywells can be used to enhance groundwater recharge by infiltrating surface runoff in surrounding soil. However, there is concern that pollutants in stormwater runoff may contaminate groundwater during drywell drainage.

Limited published research has examined the performance of drywells (Edwards, 2017; Izuka, 2011; Jurgens et al., 2008). Snyder et al. (1994) reported on a drywell recharge study in the Portland Basin in Oregon, USA, and found that 5700 drywells in urban areas contributed 38% of the total recharge to groundwater within the basin (Snyder et al., 1994). Wilson et al. (1990) analyzed the impact of drywells on recharge, groundwater pollution, and urban runoff at three sites in Arizona. Results indicated that recharge from drywells created a transmission zone for water movement with minimal impacts on groundwater quality (Wilson et al., 1990). In contrast, field and numerical modeling studies in Washington and Arizona, USA demonstrated that pollutant attenuation was related to the soil particle size, and recommended that drywells be located in soil profiles with a clay layer to enhance contaminant adsorption (Bandeen, 1984; Bandeen, 1987). In another study, Newcomer et al. (2014) reported results of both a field scale and numerical modeling studies of the effects of BMPs on groundwater recharge. In particular, the authors investigated the benefits of an infiltration trench and an irrigated lawn in San Francisco, California. (Newcomer et al., 2014). The HYDRUS-2D software (Šimůnek and van Genuchten, 2008; Šimůnek et al., 2016) was used to model the performance of experimental sites for long-term scenarios, accounting for climate change variability. Results confirmed that recharge rates beneath the infiltration trench were an order of magnitude higher than beneath the irrigation lawn, highlighting the benefits of BMPs on groundwater recharge. The above considerations suggest that, even if previous results are encouraging, more research is needed to better understand the impact of infiltration systems, such as drywells, on groundwater resources, from both a quantitative and a qualitative point of view.

Knowing the soil profile hydraulic properties is essential for the successful design, execution, and long-term operation of a potential drywell location. Therefore, numerical modeling and field scale studies need to be developed to determining average soil hydraulic properties using the inverse optimization of field scale falling head data in a modern drywell system. Most of the previous studies considered idealized homogeneous or layered soil systems. However, most field soils are highly heterogeneous, and the hydraulic conductivity may change over a short distance. Soil heterogeneity such as the presence of high and low permeable soil layers, their horizontal and vertical distribution, and connectivity significantly impacts water flow in the subsurface (Mantoglou and Gelhar, 1987; Schilling et al., 2017; Xie et al., 2014; Yeh et al., 1985b). Inadequate characterization of subsurface heterogeneity can lead to uncertainty in predicting water flow through the vadose zone, contaminant migration, and recharge estimation. Therefore, the influence of stochastic vadose zone heterogeneity on the drywell infiltration behavior and effective unsaturated soil hydraulic properties should be determined.

Most previous infiltration and recharge studies have looked at the long-term steady-state conditions when infiltration (below the root zone) equals recharge (Gray and Norum, 1967; Mantoglou and Gelhar, 1987; Yeh et al., 1985a; Yeh et al., 1985b). However, the installation of a new drywell that receives episodic water input will create transient conditions in the vadose zone that will change infiltration, recharge, and storage. In this case, infiltration will be greater than recharge until a new steady-state condition is achieved. Transient recharge behavior is important for drywells because they may not ever achieve steady-state conditions during their typical operational lifespan (e.g., a decade). However, in recent years drywells are gaining attention to be used as a MAR technique in urban, rural, and agricultural environments where a continuous water source for injection might be available. However, literature has not investigated the effect of subsurface heterogeneity on groundwater recharge from a drywell under constant head conditions, which is an upper bound (best-case scenario) for recharge and worst-case scenario for contaminant transport. In addition, identifying the arrival time and location of recharge water at the water table and its accurate monitoring is critical to assess the water quality from drywells. Microbiological contamination of groundwater can cause waterborne disease outbreaks (Feighery et al., 2013; Gunnarsdottir et al., 2013). Viruses are generally considered to be the most dangerous microbial pathogen in groundwater because they may have a low infectious dose. Contamination of groundwater by stormwater drainage wells has been reported across the U.S. (Cadmus, 1991; Cadmus, 1996; Cadmus, 1999). The residence time for a drywell depends on the setback distance between the drywell and a drinking water well. However, current regulatory guidelines to protect groundwater quality require an additional separation distance between the bottom of the drywell and the local groundwater table of 1.5 to 13 m (City of Portland, 2015; EPA, 1999; Washington State Department of Ecology, 2006). Therefore, the microbial risks from MAR techniques need to be assessed to ensure adequate protection of groundwater quality and public health. However, field scale transport experiments using pathogenic, or indicator viruses pose many technical challenges in quantifying flow and transport processes, and introduced pathogens create an unacceptable risk to human health. Therefore, there is a need to conduct numerical experiments to investigate expected virus behavior at the field scale or at specific MAR sites.

The main technical problem with drywell injection and other managed aquifer recharge approaches is clogging of the infiltration surface, leading to loss of performance and costly maintenance (Bouwer, 2002). Clogging occurs because of colloid retention and accumulation in soil pore spaces that eventually reduce porosity and permeability. Even a modest volume of retained colloids (<1% of the pore volume) can produce extreme clogging with an increased pressure drop of two to three orders of magnitude (Mays and Hunt, 2005). A variety of source waters are used for drywell injection, including treated sewage effluent and stormwater runoff from urban and rural areas. These source waters contain complex colloid suspensions (clays, silts, mineral precipitates, organic matter, and microbes) that exhibit a wide range in sizes that can induce clogging. For example, Ammann et al. (2003) investigated the effects of infiltration of urban roof runoff on a gravel-and-sand aquifer. They found a high pollution level, caused mainly by a fast breakthrough and negligible sorption of contaminants. In addition, the concentration of Total Suspended Solids (TSS) in stormwater ranges between 0.2 – 940 mg/L. This indicated that infiltration of roof runoff could increase the pollution of groundwater (Ammann et al., 2003). In addition, clogging also occurs when in situ colloids are released into infiltrating water due to changes in solution chemistry, hydrodynamic conditions, and water saturation during drywell injection (Bradford and Torkzaban, 2015; Torkzaban et al., 2015). Drywells should therefore be designed and managed to minimize such complex clogging processes. Measurement and modeling of colloid transport, retention, release, and clogging is a critical tool to help in this regard (Torkzaban et al., 2015).

Among the various MAR techniques, one of the popular systems is the infiltration basins (IBs). Infiltration basins contribute valuable technical and environmental benefits by capturing stormwater runoff and infiltrating into the underlying soil (Ferguson, 1994). They are a desirable and feasible option when the surface soil has adequate permeability, and the site has a shallow water table (Akan, 2002). They can be used to enhances groundwater recharge, reduces the peak flow and volume of water in downstream networks, limits pollution discharges to surface waters, and decreases stormwater flows in sewer systems and can be attractive to the public because they can improve urban landscapes when designed as parks or playgrounds (Dechesne et al., 2004; Dechesne et al., 2005; Dechesne et al., 2001). However, the clogging of the surface layer can reduce the infiltration capacity, and the annual cost for maintaining the surface can be expensive. In addition, the infiltration basin may not be the best feasible technique in urban areas where large open land spaces are an expensive commodity and seldom available. Therefore, there is a critical need for alternative MAR practices that can resolve challenges associated with IBs in growing urban environments. Drywells can be an alternative MAR technique for infiltration basins in an urban area. Therefore, the performance of drywells s and IBs should be assessed based on simulated values of cumulative infiltration and recharge, the number of drywells required to achieve similar or improved behavior to an IB, and the long-term operational benefits and costs.

4. Study Site

The National Training Center (NTC) at Fort Irwin, California, has been nominated through this project for initial field testing of the stormwater LID/BMP drywell technology. The NTC has experienced damaging floods in the past years. In August of 2013, the NTC received rainfall – approximately 2.5 inches in two hours – that brought significant damage to the infrastructure resulting in over $65 million in damages. Similar events were followed at the site in later years, with cumulative damage of over $160 million. Since then, the Army is trying to build infrastructures to mitigate 100-year storms. Some of the work includes existing channels, putting in rip-rap (large boulders strategically placed to break up masses of fast-flowing water in flood channels), and restoring concrete dikes and berms. They have revised the flood control plan to re-establish flood channels around Outer Loop Road and Inner Loop Road so they can better handle water rushing down from the hills behind the housing areas. The Fort Irwin cantonment area is like a giant bowl tilting northwest to southeast, and therefore, the goal is to contain water on the northeast so that it can go into established channels toward Langford Lake southeast of the cantonment area. The long-term plan is to put in retention basins along Outer Loop and Inner Loop to retain the water to recharge the water table for Fort Irwin's water wells.

The NTC sources its water from local aquifers, including the Irwin Basin, underneath the cantonment area. The Army Net Zero Water program has a long-term goal to balance water pumping with aquifer recharge, whether natural or artificial. A Net Zero Water installation's highest priority is reducing freshwater demand, followed by improving efficiency by implementing water-efficient technologies and practices. Net Zero Water installations are aimed to maximize alternative water use through recycling and reuse to reduce the demand on freshwater sources, thereby preserving the surface or groundwater sources for future use. The final step in the hierarchy is focused on recharging water back to the original water source.

A portion of the cantonment area within Fort Irwin is referred to as the Four-Plex Site (see Figure 1). Due to housing developments upstream of the recreation site, enhanced urban runoff is generated and directed into a detention/retention pond on the southwest perimeter of the four ball fields. It has been determined that a drywell has already been installed within this detention pond in early 2007. However, the catchment may take several weeks to drain the water after a significant storm event. Therefore, this site was chosen to evaluate the performance of the existing drywell, install additional drywells, assess the change in basin drainage, determine the hydraulic property of the site, and monitor the water quality and water quantity from a drywell.

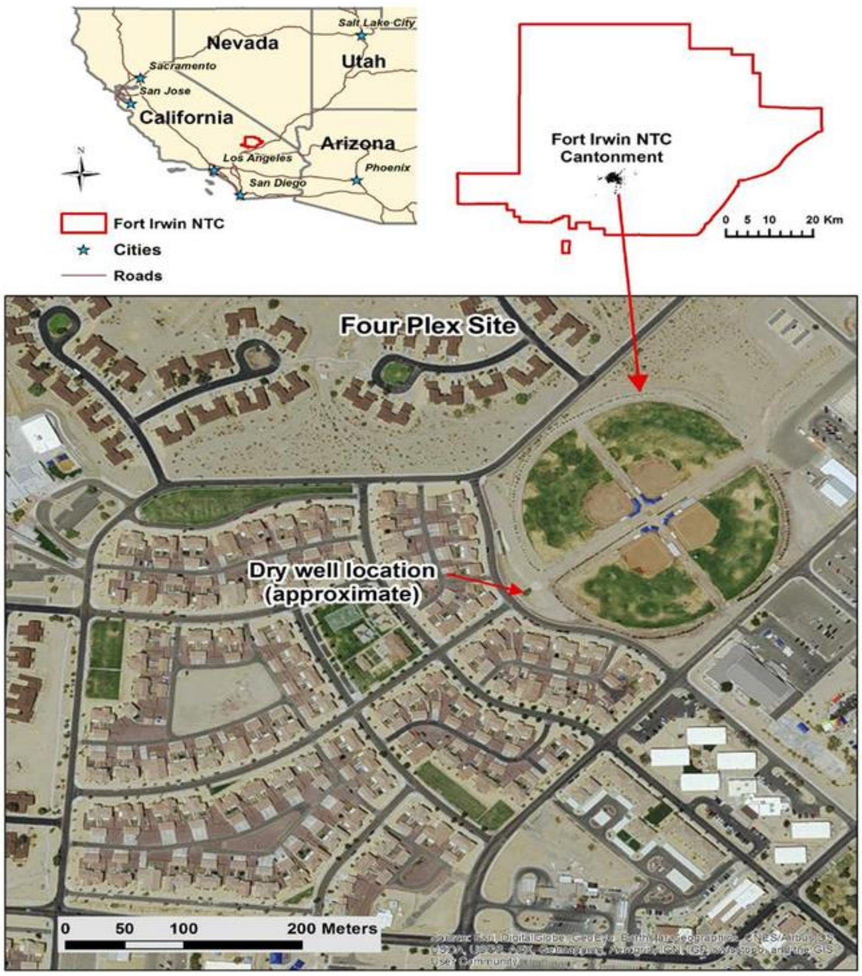

Figure 1. Location Map of Fort Irwin NTC and the Four-Plex Site.

5. Objectives

Chapter 2: Evaluating Drywells for Stormwater Management and Enhanced Aquifer Recharge

- Systematic numerical and field scale experiments were conducted to improve our understanding and ability to characterize the drywell behavior.
- The HYDRUS (2D/3D) computer software was modified to simulate transient head boundary conditions for the complex geometry of a modern drywell, i.e., a sediment chamber, an overflow pipe, and the variable geometry and storage of the drywell system with depth.
- Falling-head experiments were conducted at drywells (MaxWell IV model, Torrents Resources, Arizona, USA) located in the National Training Center in Fort Irwin, California and a commercial complex in Torrance, California.
- The effective soil hydraulic parameters with the saturated hydraulic conductivity, K_s, and the retention curve shape parameter, α, for an equivalent uniform soil system representative of both sites were determined by inverse parameter optimization of the observed falling head data.
- The fitted K_s and α parameters from these two specific sites were compared to characterize and improve the design of the drywells.

Chapter 3: Drywell Infiltration and Hydraulic Properties in Heterogeneous Soil Profiles

- The influence of subsurface heterogeneity on drywell infiltration was investigated.
- The HYDRUS (2D/3D) software was used to directly simulate cumulative infiltration volumes for selected drywell geometries and soil heterogeneities under constant or falling head conditions.
- Subsurface heterogeneity was described in this model deterministically by defining soil layers or lenses, or by generating stochastic realizations of soil hydraulic properties with selected variance and correlation lengths.
- The numerically generated data were then used in inverse optimizations to determine the hydraulic properties and lateral extension of individual layers or lenses or determine soil hydraulic properties of an equivalent homogeneous profile.
- The influence of stochastic subsurface heterogeneity parameters (e.g., the variance, horizontal, and vertical correlation length) on cumulative drywell infiltration and equivalent homogeneous profile values of K_s and α were determined.

Chapter 4: Groundwater Recharge from Drywells Under Constant Head Conditions

- This study investigated the influence of subsurface heterogeneity on groundwater recharge from a drywell, especially the short-term condition when recharge does not yet equal infiltration.

- The HYDRUS (2D/3D) software was used to directly simulate cumulative infiltration and recharge volumes from a drywell for different homogenous and heterogeneous soils.
- Constant head conditions were considered in the drywell to facilitate the determination of subsurface soil properties on the upper limit for recharge (and contaminant transport) and the lower limit on arrival time.
- Subsurface heterogeneity was described in this model by generating stochastic realizations of soil hydraulic properties with selected standard deviation, and vertical and horizontal correlation lengths.
- The influence of stochastic subsurface heterogeneity parameters on cumulative infiltration (I) and recharge (R) volumes, the radius of recharge (r_x), early (EAT) and late (LAT) arrival times, and early (EAP) and late (LAP) arrival points were determined to understand the drywell infiltration and recharge behavior in the deep vadose zone (60 m).

Chapter 5: Virus Transport from Drywells Under Constant Head Conditions: A Modeling Study

- This study was conducted to demonstrate the application of numerical experiments using HYDRUS (2D/3D) software coupled with column laboratory-scale data to understand the influence of subsurface heterogeneity on virus transport, where field scale studies are not feasible.
- Constant head water flow simulations were conducted to obtain steady-state initial conditions in the flow domain to represent the worst-case scenario for virus transport.
- Additional constant head simulations for virus transport were considered in a drywell to understand the effect of various removal parameters on virus transport under homogenous and different subsurface heterogeneity conditions.

Chapter 6: Comparison of Recharge from Drywells and Infiltration Basins: A Modeling Study

- This study was conducted to compare groundwater recharge from drywells and IBs under various homogeneous and heterogeneous subsurface conditions.
- The HYDRUS (2D/3D) software was used to directly simulate cumulative infiltration and recharge volumes from drywells and IBs.
- Constant head conditions were considered in drywells and IBs to determine the comparable upper limit for recharge.
- Subsurface heterogeneity was described in this model by generating stochastic realizations of soil hydraulic properties.
- The performance of drywells and IBs were assessed based on simulated values of cumulative infiltration and recharge, the number of drywells

required to achieve similar or improved behavior to an IB, and the long-term operational benefits and costs.

- The use of the numerical model tool to screen MAR designs for a specific site application was explored.

Chapter 7: Site-specific Analysis of Drywell I, Drywell II, Vadose Zone Monitoring Well, Perched Water Table, and Groundwater Table

- This chapter summarizes the overall functioning of the catchment basin, old drywell (Drywell I), new drywell (Drywell II), the perched water table, monitoring well, and groundwater table at the Fort Irwin Basin.
- The daily inflow of irrigation overflow, the subsequent water flow dynamics of Drywell I, its sedimentation chamber (SC1), lower chamber/spillover well (DW1), the connection pipe, Drywell II, and its sedimentation chamber (SC2) and lower chamber (DW2) were assessed.
- The hydraulic performance of DW1 and DW2 was assessed to understand the short-term and long-term infiltration behavior and loss of infiltration capacity due to clogging.
- Turbidity measurements in SC1 and SC2 were analyzed to evaluate the MaxWell Plus drywell design and its impact on injection water-sediment load.
- The water level for the perched water table formed above a clay layer at the site was assessed to understand its slow response to infiltration and rain event.
- The vadose monitoring data (water content, electrical conductivity, and temperature) were analyzed to understand the water flow above and below the perched water table and its recharge behavior.
- Water level data in the groundwater table was analyzed to understand the change in response to pumping and recharge events.
- Representative rain event data were investigated in detail to demonstrate the complete flow dynamics of the catchment basin, drywell systems, perched water table, and groundwater.

CHAPTER 2

Evaluating Drywells for Stormwater Management and Enhanced Aquifer Recharge

Published Manuscript: Sasidharan S, Bradford SA, Šimůnek J, DeJong B, Kraemer SR. Evaluating drywells for stormwater management and enhanced aquifer recharge. Advances in water resources. 2018 June 1;116:167-77.
https://doi.org/10.1016/j.advwatres.2018.04.003

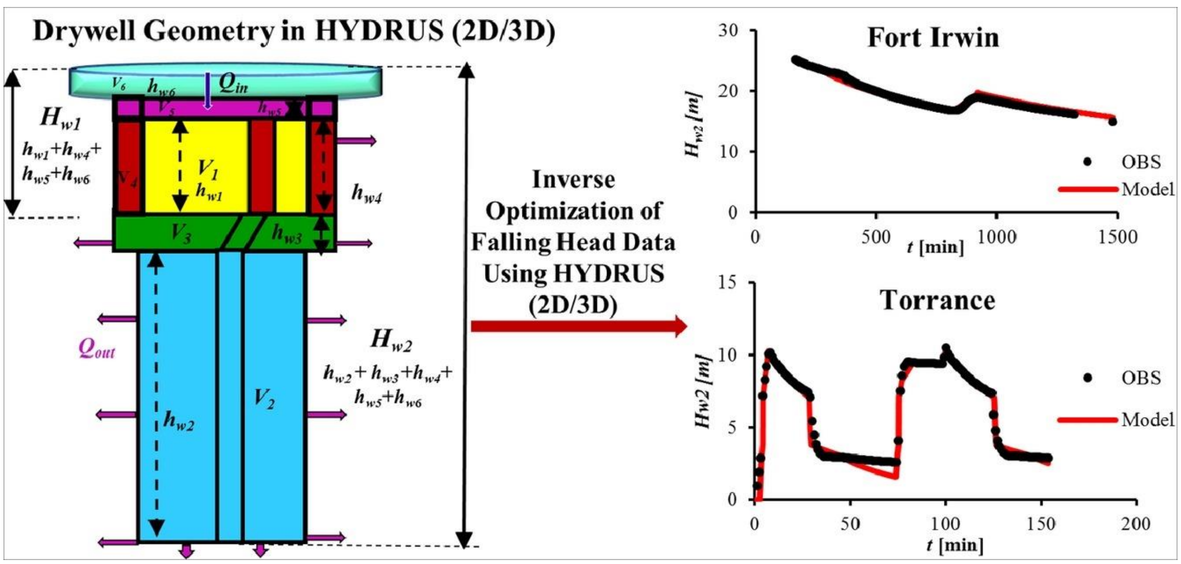

ABSTRACT

Drywells are increasingly used for stormwater management and enhanced aquifer recharge, but only limited research has quantitatively determined the performance of drywells. Numerical and field-scale experiments were, therefore, conducted to improve our understanding and ability to characterize the drywell behavior. In particular, HYDRUS (2D/3D) was modified to simulate transient head boundary conditions for the complex geometry of the Maxwell Type IV drywell; i.e., a sediment chamber, an overflow pipe, and the variable geometry and storage of the drywell system with depth. Falling-head infiltration experiments were conducted on drywells located at the National Training

Center in Fort Irwin, California (CA) and a commercial complex in Torrance, CA to determine in situ soil hydraulic properties (the saturated hydraulic conductivity, Ks, and the retention curve shape parameter, α) for an equivalent uniform soil profile by inverse parameter optimization. A good agreement between the observed and simulated water heights in wells was obtained for both sites as indicated by the coefficient of determination 0.95-0.99–%, unique parameter fits, and small standard errors. Fort Irwin and Torrance drywells had very distinctive soil hydraulic characteristics. The fitted value of K_s=1.01 × 10−3 m min−1 at the Torrance drywell was consistent with the sandy soil texture at this site and the default value for sand in the HYDRUS soil catalog. The drywell with this K_s= 1.01 × 10−3 m min−1 could easily infiltrate predicted surface runoff from a design rain event (~51.3 m3) within 5760 min (4 d). In contrast, the fitted value of K_s=2.25 × 10−6 m min−1 at Fort Irwin was very low compared to the Torrance drywell and more than an order of magnitude smaller than the default value reported in the HYDRUS soil catalog for sandy clay loam at this site, likely due to clogging. These experiments and simulations provide useful information to characterize effective soil hydraulic properties in situ, and to improve the design of drywells for enhanced recharge.

Note: The free article can be accessed from the PubMed webpage

CHAPTER 3

Drywell Infiltration and Hydraulic Properties in Heterogeneous Soil Profiles

Published Manuscript: **Sasidharan S, Bradford SA, Šimůnek J, Kraemer SR. Drywell infiltration and hydraulic properties in heterogeneous soil profiles. Journal of hydrology. 2019 Mar 1;570:598-611.**
https://doi.org/10.1016/j.jhydrol.2018.12.073

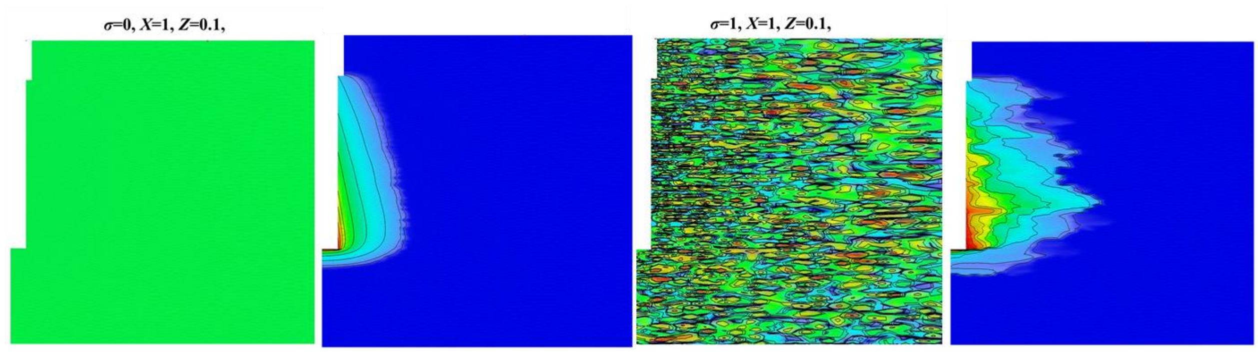

ABSTRACT

Drywells are increasingly used to capture stormwater runoff for surface infiltration and aquifer recharge, but little research has examined the role of ubiquitous subsurface heterogeneity in hydraulic properties on drywell performance. Numerical experiments were therefore conducted using the HYDRUS (2D/3D) software to systematically study the influence of subsurface heterogeneity on drywell infiltration. Subsurface heterogeneity was described deterministically by defining soil layers or lenses, or by generating stochastic realizations of soil hydraulic properties with selected variance (σ) and horizontal (X) and vertical (Z) correlation lengths. The infiltration rate increased when a high permeability layer/lens was located at the bottom of the drywell, and had larger vertical and especially horizontal dimensions. Furthermore, the average cumulative infiltration (I) for 100 stochastic realizations of a given subsurface heterogeneity increased with σ and X, but decreased with Z. This indicates that the presence of many highly permeable, laterally extending lenses provides a larger surface area for enhanced infiltration than the presence of isolated, highly permeable lenses. The ability to inversely

determine soil hydraulic properties from numerical drywell infiltration results was also investigated. The hydraulic properties and the lateral extension of a highly permeable lens could be accurately determined for certain idealized situations (e.g., simple layered profiles) using constant head tests. However, variability in soil hydraulic properties could not be accurately determined for systems that exhibited more realistic stochastic heterogeneity. In this case, the heterogeneous profile could be replaced with an equivalent homogeneous profile and values of an effective isotropic saturated conductivity (Ks) and the shape parameter in the soil water retention function (α) could be inversely determined. The average value of Ks for 100 stochastic realizations showed a similar dependency to I on σ, X, and Z. Whereas, the average value of α had large confidence interval for soil heterogeneity parameters and played a secondary role in drywell infiltration. This research provides valuable insight on the selection of site, design, installation, and long-term performance of a drywell.

Note: The free article can be accessed from the PubMed webpage

CHAPTER 4

Groundwater Recharge from Drywells Under Constant Head Conditions

Published Manuscript: Sasidharan S, Bradford SA, Šimůnek J, Kraemer SR. Groundwater recharge from drywells under constant head conditions. Journal of hydrology. 2020 April 1;583:124569. https://doi.org/10.1016/j.jhydrol.2020.124569

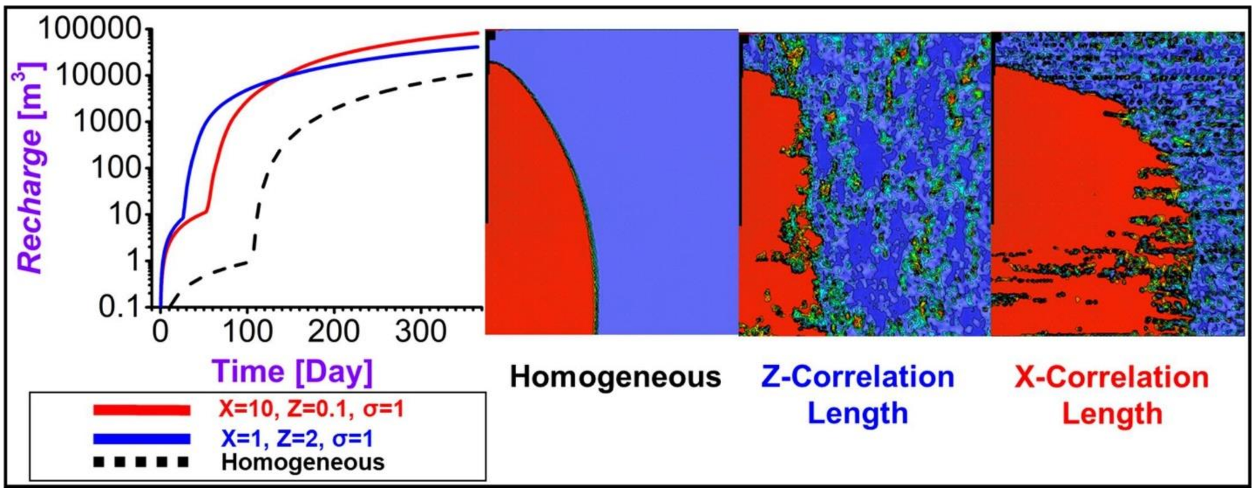

ABSTRACT

Drywells are widely used as managed aquifer recharge devices to capture stormwater runoff and recharge groundwater, but little research has examined the role of subsurface heterogeneity in hydraulic properties on drywell recharge efficiency. Numerical experiments were therefore conducted on a 2D-axisymmetric domain using the HYDRUS (2D/3D) software to systematically study the influence of various homogenous soil types and subsurface heterogeneity on recharge from drywells under constant head conditions. The mean cumulative infiltration (μI) and recharge (μR) volumes increased with an increase in the saturated hydraulic conductivity (K_S) for various homogeneous soils. Subsurface heterogeneity was described by generating ten stochastic realizations of soil hydraulic properties with selected standard deviation (σ),

and horizontal (*X*) and vertical (*Z*) correlation lengths. After 365 days, values of *μI, μR*, and the radius of the recharge area increased with *σ* and *X* but decreased with *Z*. The value of *μR* was always smaller for a homogeneous than a heterogeneous domain. This indicates that recharge for a heterogeneous profile cannot be estimated with an equivalent homogeneous profile. The value of *μR* was always smaller than *μI* and correlations were highly non-linear due to vadose zone storage. Knowledge of only infiltration volume can, therefore, lead to misinterpretation of recharge efficiency, especially at earlier times. The arrival time of the wetting front at the bottom boundary (60 m) ranged from 21-317 days, with earlier times occurring for increasing *σ* and *Z*. The corresponding first arrival location can be 0.1-44 m away from the bottom releasing point of a drywell in the horizontal direction, with greater distances occurring for increasing *σ* and *X*. This knowledge is important to accurately assess drywell recharged performance, water quantity, and water quality.

Note: The free article can be accessed from the PubMed webpage

CHAPTER 5

Virus Transport from Drywells Under Constant Head Conditions: A Modeling Study

Published Report: Sasidharan, S., Bradford, S.A., Šimůnek, J. and Kraemer, S.R., 2021. Virus transport from drywells under constant head conditions: A modeling study. Water Research, 197, p.117040. https://doi.org/10.1016/j.watres.2021.117040

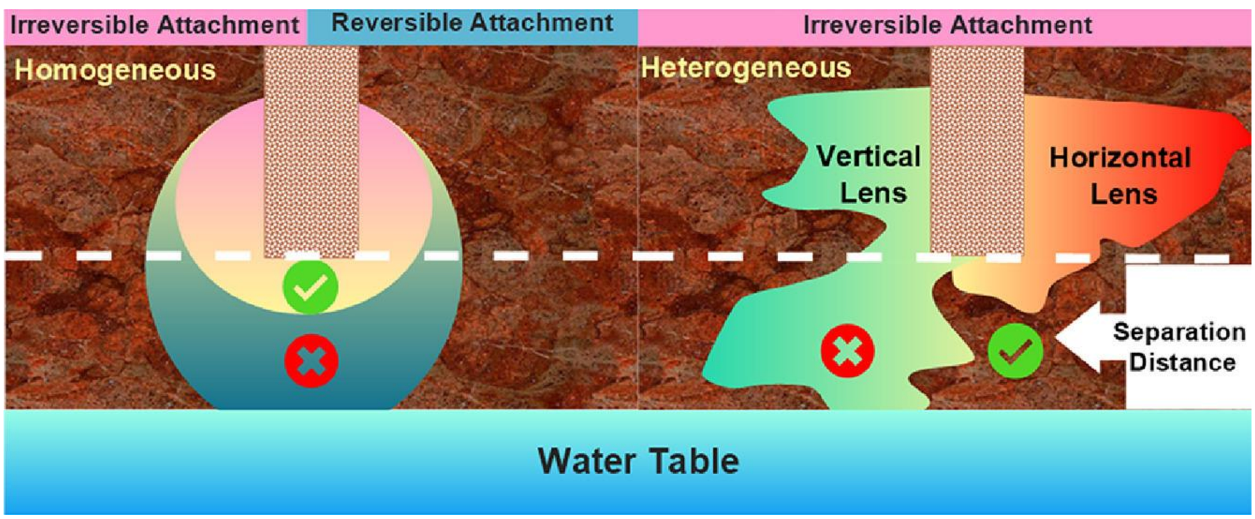

ABSTRACT

Many arid and semi-arid regions of the world face challenges in maintaining the water quantity and quality needs of growing populations. A drywell is an engineered vadose zone infiltration device widely used for stormwater capture and managed aquifer recharge. To our knowledge, no prior studies have quantitatively examined virus transport from a drywell, especially in the presence of subsurface heterogeneity. Axisymmetric numerical experiments were conducted to systematically study virus fate from a drywell for various virus removal and subsurface heterogeneity scenarios under steady-state flow conditions from a constant head reservoir. Subsurface domains were homogeneous or had stochastic heterogeneity with selected standard deviation (σ) of lognormal distribution in saturated hydraulic conductivity and horizontal (X) and vertical (*Z*) correlation lengths.

Low levels of virus concentration tailing can occur even at a separation distance of 22 m from the bottom of the drywell, and 6-log_{10} virus removal was not achieved when a small detachment rate (kd_1=1 × 10^{-5} min^{-1}) is present in a homogeneous domain. Improved virus removal was achieved at a depth of 22 m in the presence of horizontal lenses (e.g., X=10 m, Z=0.1 m, σ=1) that enhanced the lateral movement and distribution of the virus. In contrast, faster downward movement of the virus with an early arrival time at a depth of 22 m occurred when considering a vertical correlation in permeability (X=1 m, Z=2 m, σ=1). Therefore, the general assumption of a 1.5–12 m separation distance to protect water quality may not be adequate in some instances, and site-specific microbial risk assessment is essential to minimize risk. Microbial water quality can potentially be improved by using an in situ soil treatment with iron oxides to increase irreversible attachment and solid-phase inactivation.

Note: The free article can be accessed from the PubMed webpage after 1 year.

CHAPTER 6

Comparison of Recharge from Drywells and Infiltration Basins: A Modeling Study

Published Manuscript: **Sasidharan S, Bradford SA, Šimůnek J, Kraemer SR. Comparison of recharge from drywells and infiltration basins: A modeling study. Journal of Hydrology. 2021 March 1;594:125720.**
https://doi.org/10.1016/j.jhydrol.2020.125720

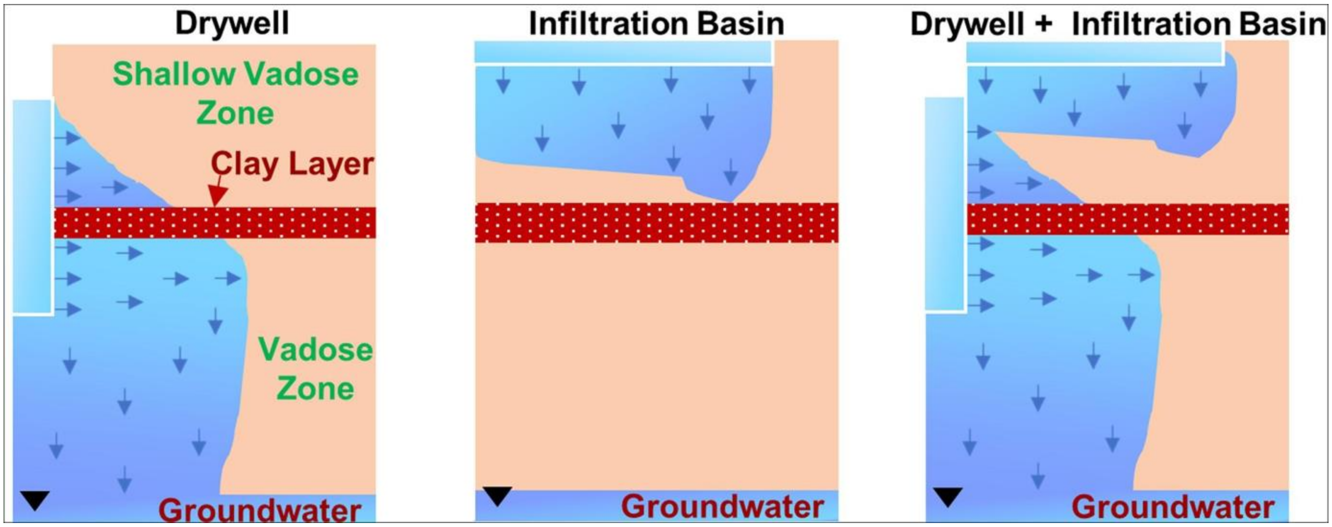

ABSTRACT

Drywells (DWs) and infiltration basins (IBs) are widely used as managed aquifer recharge (MAR) devices to capture stormwater runoff and recharge groundwater. However, no published research has compared the performance of these two engineered systems under shared conditions. Numerical experiments were conducted on an idealized 2D-axisymmetric domain using the HYDRUS (2D/3D) software to systematically study the performance of a circular IB design (diameter and area) and partially penetrating DW (38 m length with water table > 60 m). The effects of subsurface heterogeneity on infiltration, recharge, and storage from the DW and IB under constant head conditions were investigated. The mean cumulative infiltration (μI) and recharge (μR) volumes increased, and the arrival time of recharge decreased with the IB area. Values of μI were

higher for a 70 m diameter IB than an DW, whereas the value of *μR* was higher for a DW after 1-year of a constant head simulation under selected subsurface heterogeneity conditions. A comparison between mean *μI*, *μR*, and mean vadose zone storage (*μS*) values for all DW and IB stochastic simulations (70 for each MAR scenario) under steady-state conditions demonstrated that five DWs can replace a 70 m diameter IB to achieve significantly higher infiltration and recharge over 20 years of operation. Additional numerical experiments were conducted to study the influence of a shallow clay layer by considering an IB, DW, and a DW integrated into an IB. The presence of such a low permeable layer delayed groundwater recharge from an IB. In contrast, a DW can penetrate tight clay layers and release water below them and facilitate rapid infiltration and recharge. The potential benefits of a DW compared to an IB include a smaller footprint, the potential for pre-treatments to remove contaminants, less evaporation, less mobilization of in-situ contaminants, and potentially lower maintenance costs. Besides, this study demonstrates that combining both IB and DW helps to get the best out of both MAR techniques.

Note: The free article can be accessed from the PubMed webpage after 1 year.

CHAPTER 7

Fort Irwin Site Research Summary:

Site-specific Analysis of Drywell I, Drywell II, Vadose Zone Monitoring Well, Perched Water Table, and Groundwater Table

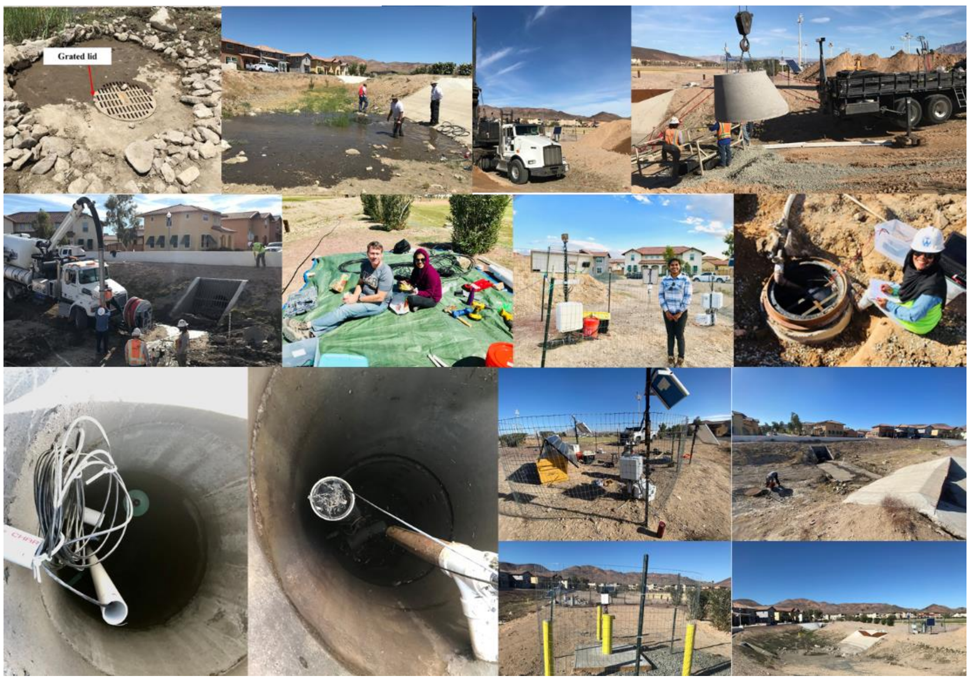

7.1. Drywells at Fort Irwin, CA

The Fort Irwin site has two drywells (DW), one monitoring well (MW), and a test well (TW). The first drywell (DW1) was installed in 2007 prior to the initiation of this study and the second drywell (DW2) was installed in December 2018. This study focuses on the events during the project period from January 2017 to July 2021. In addition, several other research activities were conducted at the site during this period, and a short synopsis of events is presented as Figs. 1–9.

DW1 was found submerged under sediments and soil within the basin during a site visit in early 2016. The lack of maintenance led to the accumulation of sediments in the drywell and poor drainage. The basin would take a few weeks to drain the captured stormwater. In the June 2017 visit, the cement pad around the grated lid was cleaned, and rocks were placed around the well to minimize further entry of sediments and trash into the DW1. Fig.1A shows the grated lid for the DW1 after cleaning. A falling head experiment was conducted to determine the soil hydraulic properties of DW1 by flooding the basin using a fire hydrant. The methods and results are explained in detail in Sasidharan et al. (2018) (Chapter 2). The US EPA installed a test well on November 12, 2018, to further characterize the site's soil hydraulic properties (Fig. 2).

DW2 was installed in December 2018 to improve the basin's drainage function during summer and winter storms, mitigate local flood damage, and enhance aquifer recharge. DW1 and DW2 were connected with a 6" pipe to upgrade the original Torrent Resources MaxWell IV drywell design for DW1 to a MaxWell Plus system (Fig. 3). During this activity, the DW1's sedimentation chamber (SC1) was cleaned using a vacuum truck to remove all the accumulated sediments from the bottom of the SC1. The cap for the overflow pipe in the SC1 (OVF1) was found at the bottom of the SC1 and was recovered and placed on the OVF1 (Fig. 4). An attempt was made to perform a constant head and falling head experiment in DW2 by pumping water directly into the DW2 sedimentation chamber (SC2). However, the infiltration rate from SC2 was so high that we could not maintain a constant head condition (Fig. 5).

All the drywells were equipped with various monitoring sensors to measure these systems' performance on April 2, 2019. The SC1 and SC2 were instrumented with OBS3+ turbidity sensor (Campbell Scientific, USA) and a CS451 pressure transducer (Campbell Scientific, USA). The lower chamber of DW1 and DW2 was also equipped with a CS451 pressure transducer. The OBS3+ sensor comes with a stainless-steel body to be used in freshwater with a maximum submersion depth of 500 m. It has a diameter of 2.5 cm and a height of 14.1 cm. It can operate in a temperature range of 0° to 40°C. The OBS3+ sensor was monitored using a CR23X datalogger from Campbell Scientific. The OBS3+ sensor has one channel with the 4-20 mA output to measure the lower turbidity range (0-1000 NTU) and another channel with a 0 to 5 V output to measure the higher turbidity range (0-4000 NTU) with an accuracy of 2% or 0.5 NTU. The concentration range for mud is 5,000-10,000 mg L^{-1} with an accuracy of 2% or 1 mg L^{-1} and for sand is 50,000-100,000 mg L^{-1} with an accuracy of 4% or 10 mg L^{-1}. (Campbell Scientific, USA) The CS451 consists of a piezoresistive sensor housed in a 316L stainless-steel package to enhance reliability. The rugged construction makes the CS451 sensor suitable for water level measurement in irrigation applications, water wells, lakes, streams, and tanks. The cable incorporates a vent tube to compensate for atmospheric pressure fluctuations, and the jacket is made of rugged Hytrel®, designed to remain flexible and tough, even under harsh environmental conditions. The CS451 operates over a water depth range of 0-50.9 m (500 kPa) with a resolution of 0.0035% FS and accuracy of 0.1%. The operating temperature ranges from 0 to 60 °C, and the power requirement is 5-18 VDC (an internal user-replaceable lithium battery with 5+ years lifespan when the logging interval is once per hour). The sensor has a dimension of 21.3 cm (L) × 2.1 cm (W). The sensor was connected to a CR23X datalogger, and the data was collected and analyzed using the LoggerNet software. In addition, the datalogger was connected to a battery and solar panel for continuous data acquisition and a cellular modem for remote access of data using the Campbell Scientific LoggerNet Software (Fig. 6). All the sensors in both drywells collected sensor measurements at every minute.

The cover for the OVF1 was once again found on the floor of SC1 during a site visit on April 2, 2019. We, therefore, covered the OVF1 using a mesh to prevent any further addition of trash and minimize addition of sediments. During the annual visit on January 13, 2020, the cement pad surrounding the DW1 and all the sensors in SC1 were found to be covered with sediments. The cement pad was cleaned, and the DW1 was protected using rocks, and all the sensors were cleaned and placed 1 m above the bottom of the SC1 and SC2 (Fig. 7). On December 11, 2019, Geo System Analysis completed a monitoring well (MW) equipped with vadose zone monitoring sensors at various depths and groundwater level sensors (Fig. 9). All the details on the MW can be found in the GeoSystem Analysis Report (Milczarek et al., 2020). In addition, UC Riverside and USDA conducted several annual visits for site maintenance (Fig. 9). However, the reoccurring presence of sediments and trash in the basin demonstrates that the Army should conduct more frequent maintenance to maintain and expand the lifespan of drywells at the site.

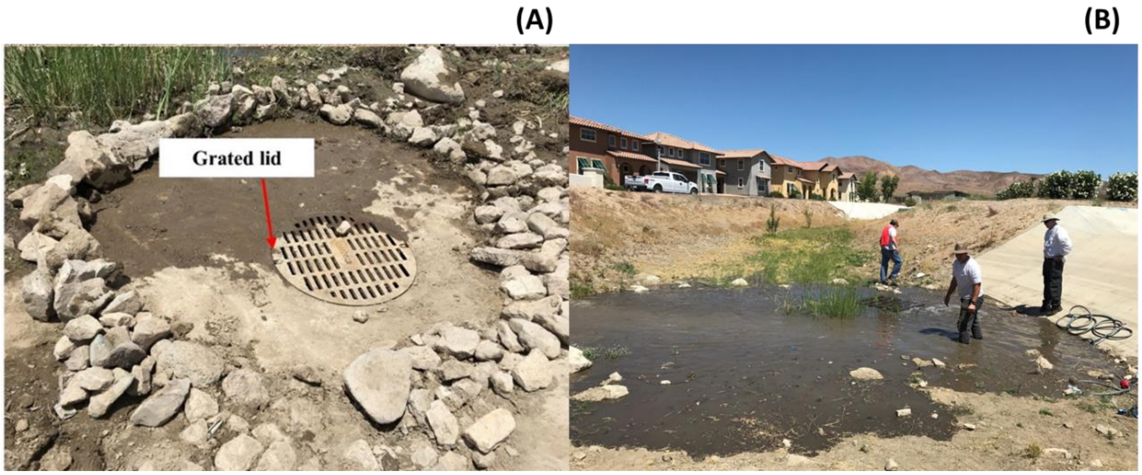

Figure 1. The DW1 **(A)** and the falling head test was conducted by flooding the basin using a fire hydrant and filling and draining DW1 on June 5, 2017 (Sasidharan et al., 2018) **(B)**, by UC Riverside and USDA Riverside.

Figure 2. The installation of a test well to measure the site soil hydraulic properties on November 12, 2018, by the US EPA.

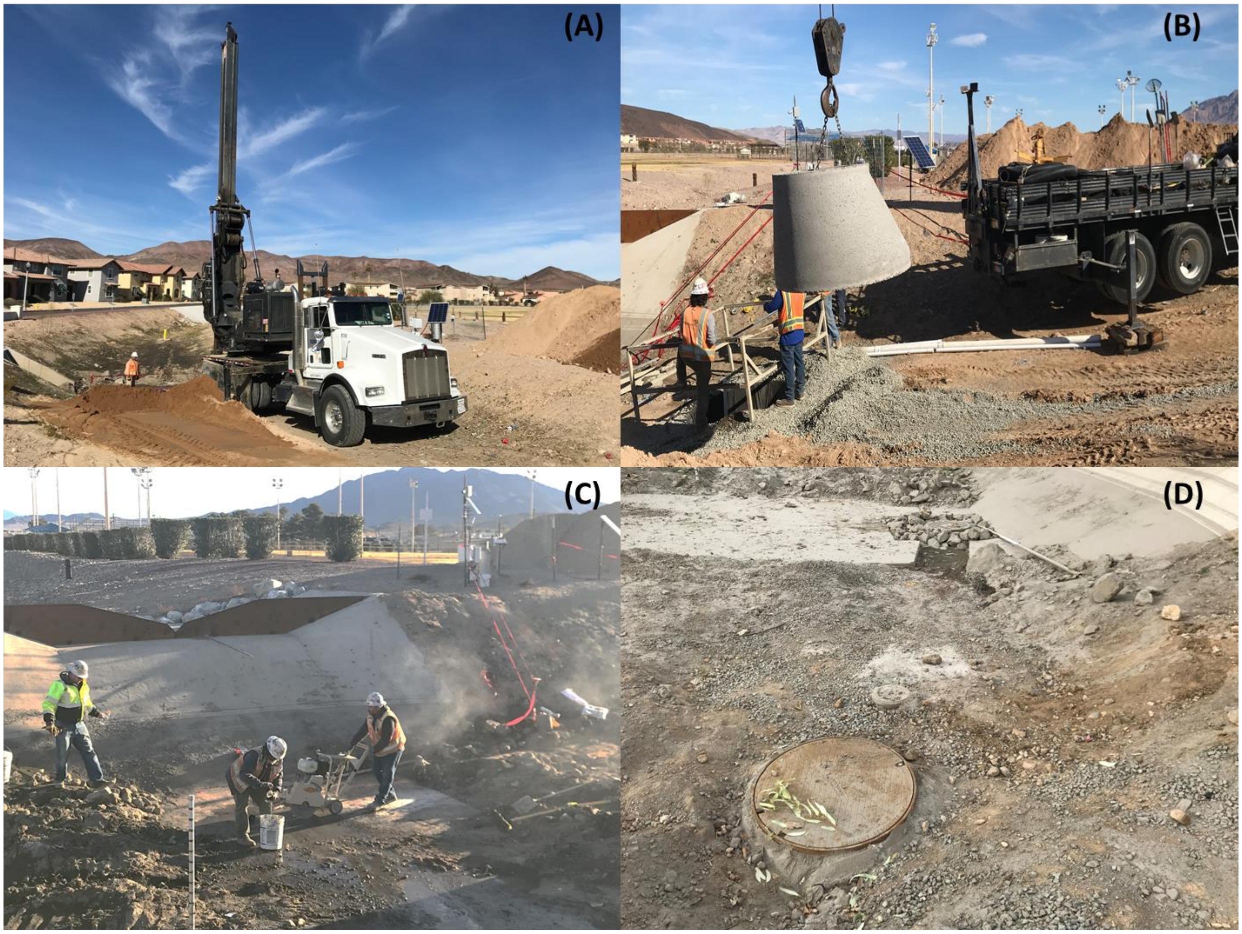

Figure 3. The installation of DW2 **(A & B)** and connection pipe **(C)** and completed well **(D)** at Fort Irwin on December 17th – 21st, 2018 by Torrent Resources, UC Riverside, and USDA Riverside.

Figure 4. The DW1 sedimentation chamber (SC1) before cleaning where the cap for the overflow pipe is fallen and, on the floor, **(A)**. Army site contractors cleaned SC1 using a vacuum truck on December 19, 2018 **(B)**.

Figure 5. Performing a falling head test by connecting water from a fire hydrant to DW2's sedimentation chamber (SC2) to measure the hydraulic properties of the site on December 20, 2018, by Torrent Resources, UC Riverside, and USDA Riverside.

Figure 6. Installation of sensors and equipment (water level, turbidity, and remote data access) to continuously monitor the performance of drywells **(A, B, &C)**, the restored SC1 with a permeable net cap on overflow pipe, sensors, and connection pipe in SC1 **(D)**, sensors, sensor tube, piezometer tube, and connection pipes in SC2 **(E)**, and the complete automated operational site on April 2, 2019, monitored by UC Riverside, and USDA Riverside. All the sensors are placed at the bottom of the respective chambers, i.e., SC1, SC2, DW1, and DW2.

Figure 7. Completed monitoring well (MW) by GeoSystem Analysis on December 11, 2019, and data collection and maintenance by UC Riverside and USDA Riverside.

Figure 8. The drywell and the surrounding cement pad **(A),** SC1 **(B)**, and the sensors **(C)** covered with sediments were observed during the annual site maintenance visit on January 13, 2020. All the sensors were cleaned and placed 1 m above from the bottom of the SC1 and SC2, and the cement pad was cleaned, and the DW1 was protected using rocks by UC Riverside and USDA Riverside.

Figure 9. Annual site visit and maintenance were conducted on November 12, 2020 **(A),** and May 4, 2021 (B) by UC Riverside.

The design and various modeling aspects of DW1 and DW2 are explained in detail in Chapter 2 (Sasidharan et al., 2018) and Chapter 4 (Sasidharan et al., 2020), respectively. Figure 10 and 11 shows the DWs design, the connection pipes, and the current location of the sensors. In brief, the MaxWell IV model (Torrents Resources, Phoenix, Arizona, USA) drywell was installed at Fort Irwin. According to the engineered design, the DW1 receives inflow water into an upper sedimentation chamber (SC1) through a grated opening on top. This upper sediment chamber has an impermeable chamber sidewall with perforations (small holes), a concrete base seal, and a floating hydrocarbon capture pillow, which removes a wide range of hydrocarbons. Silt, sediment, and debris settle out of the water by gravity inside the upper chamber. Incoming water rises inside the upper sediment chamber and then enters an overflow intake pipe connected to a lower chamber (DW1). The overflow inlet is equipped with a debris screen, which blocks the passage of suspended matter and other floating debris. Water from the overflow pipe enters a lower chamber filled with clean rocks (0.9–3.8 cm). The entire gravel pack is surrounded by a fully permeable (needle punched) non-woven geotextile (polypropylene or polyester) fabric sleeve to prevent the migration of fines into the gravel pack. Water in the gravel pack infiltrates into the vadose zone soil envelope and eventually recharges groundwater aquifers. Once the SC1 fills up, and when the water reaches the connection pipe, it enters the SC2 and will overflow through the overflow pipe (OVF2) and fills DW2, and water infiltrates into the surrounding soil. Figure 12 shows the geometry of the DW1 based on the Torrent Resources completion document. However, based on the on-site measurements in June 2017, the sedimentation chamber (SC1) was filled with 1.129 m of sediments, and therefore, the depth was reduced from 4.6 m to 3.471. Subsequently, the SC1 was cleaned in December 2018, and the SC1 depth was restored to the original 4.6 m. Fig. 13 shows the schematic of the DW2.

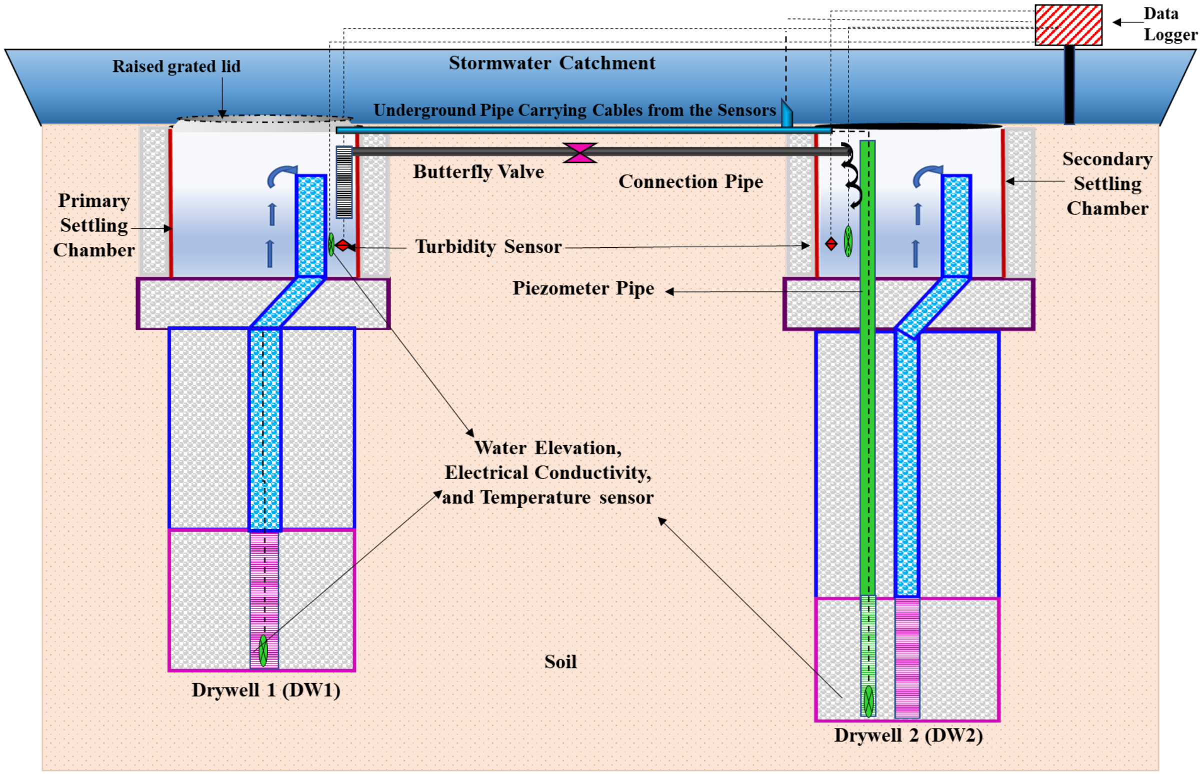

Figure 10. A schematic of the catchment basin, DW1, DW2, the connection pipes, sensors, and the monitoring station at the Fort Irwin Site, CA.

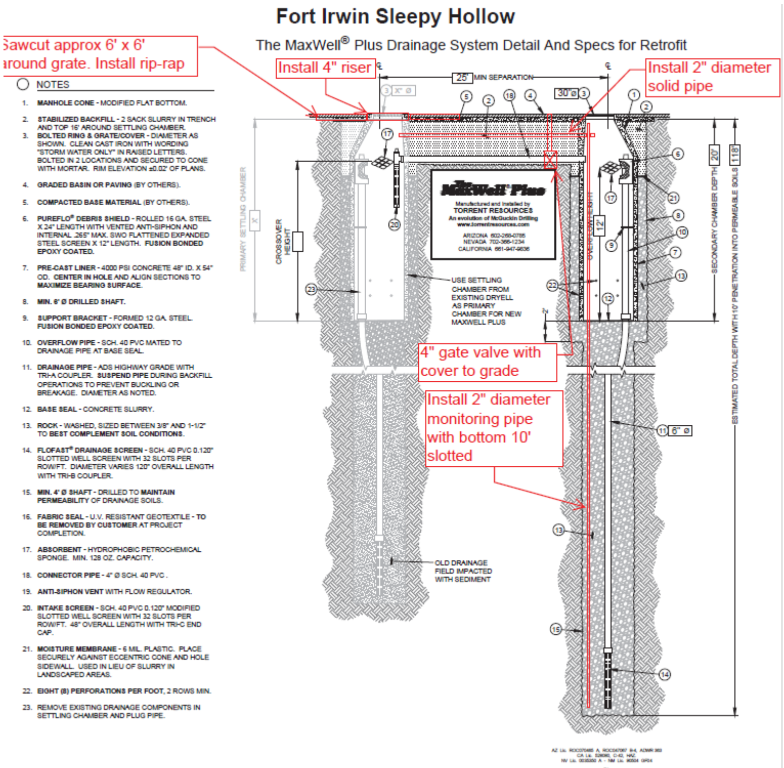

Figure 11. The completed DW1, DW2, and the connection pipe schematic by Torrent Resources.

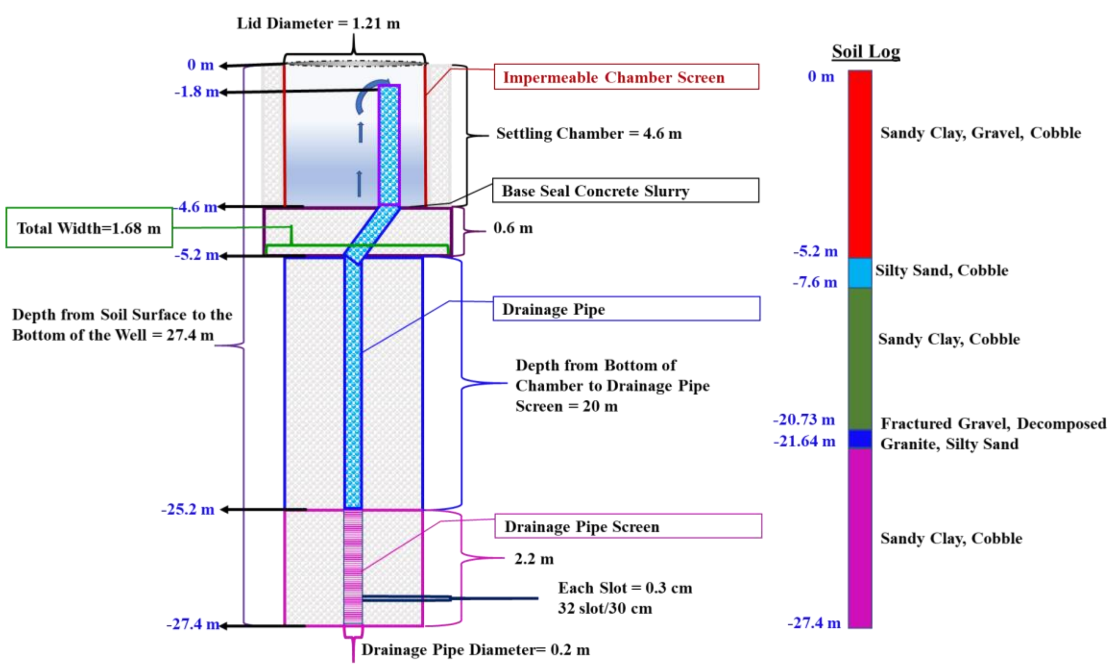

Figure 12. The DW1's geometry and soil log information based on the Torrent Resources completion document in 2007.

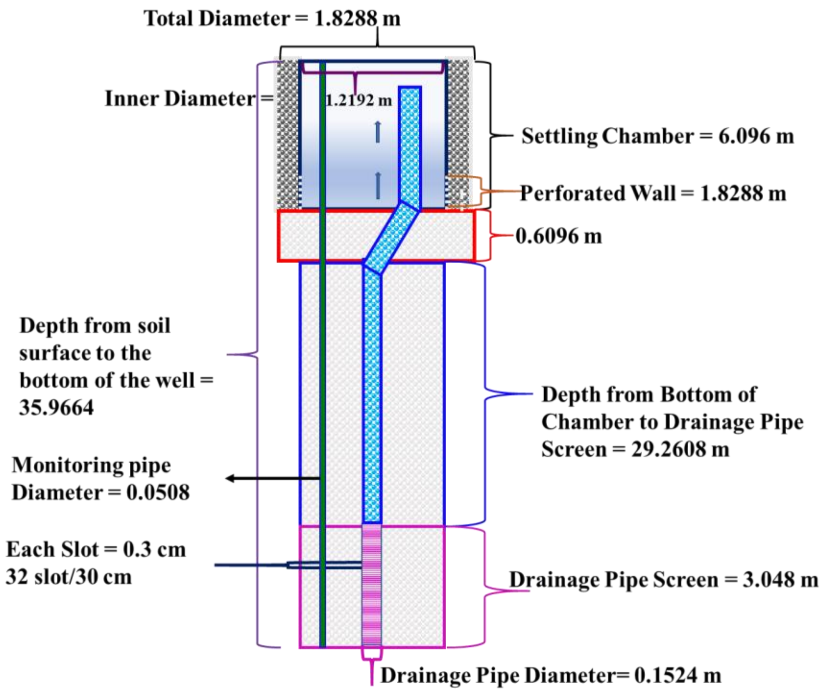

Figure 13. The DW2's geometry information based on the Torrent Resources completion document in December 2018, and UC Riverside and USDA Riverside direct site measurement in April 2019.

7.2. Daily Inflow and Drywell Flow Dynamics

The Fort Irwin site receives a nightly inflow of about 1–43 m^3 of water (Sasidharan et al., 2020) into the sedimentation chamber from outdoor irrigation runoff at the housing development. Fig. 14 shows the monitoring data for the period of 04/12/2019-06/29/2021 that totals 819 days. The overflow pipe in SC1 (OVF1) is 2.8 m, and the overflow pipe in SC2 (OVF2) is 3.7 m. The connection pipe is 3.6 m from the bottom of SC1. Figs. 14A and 14B show the daily inflow of water in SC1 and DW1. A nearly constant head condition was maintained in DW1 (Sasidharan et al., 2020) because clogging of the lower chamber created a low saturated conductivity equaled 2.25×10^{-6} m min^{-1} in the soil around DW1 (Sasidharan et al., 2018).

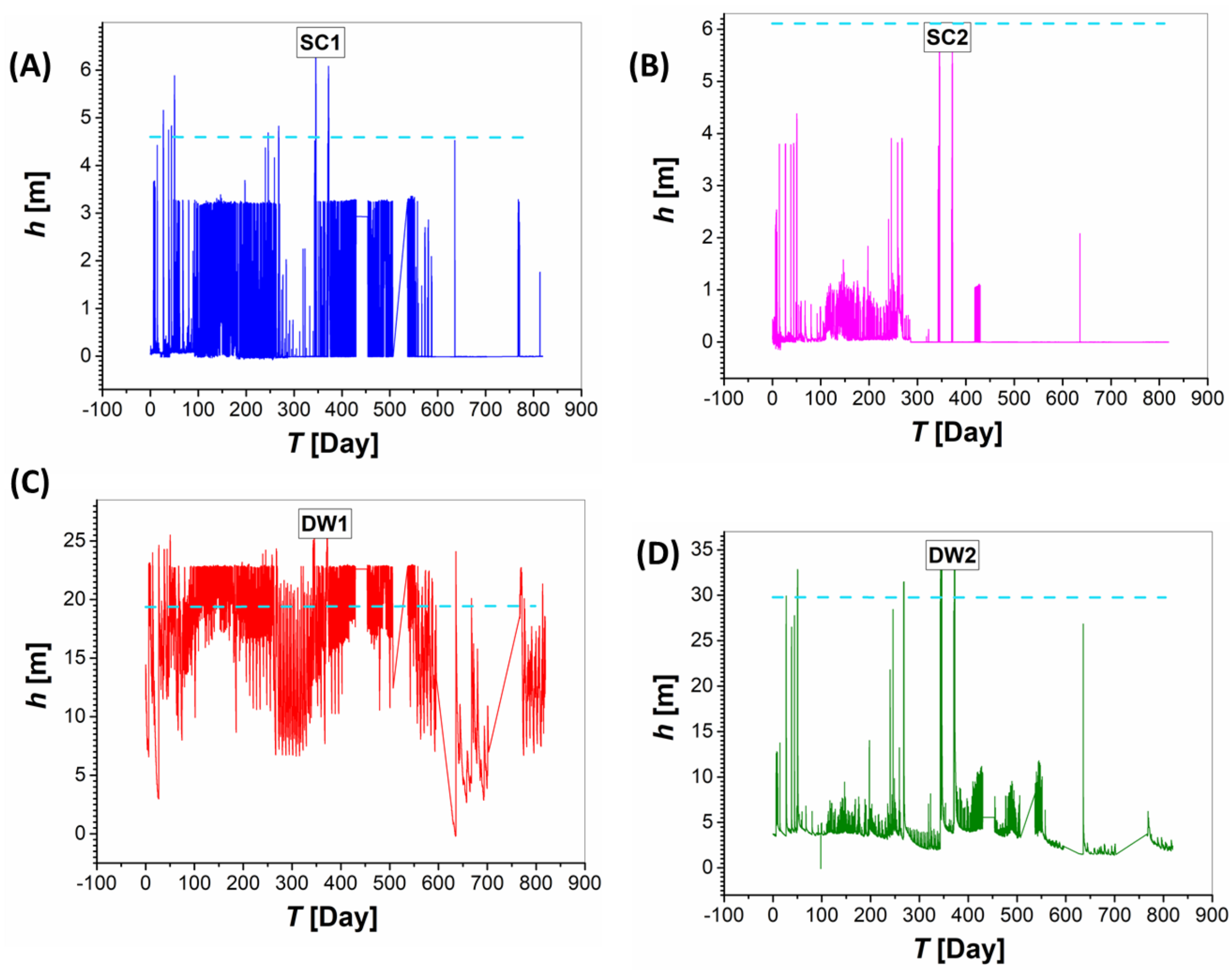

Figure 14. The daily water inflow into SC1 **(A)**, SC2 **(B)**, DW1 **(C)**, and DW2 **(D)** during the period of 04/12/2019-06/29/2021.

Fig. 14 shows that data collection was interrupted a few times due to a connection failure or battery drain, and site inaccessibility because of the global COVID-19 pandemic in 2020. This data interruption is reflected in Fig. 14 as gaps that are summarized in Table 1. In addition, on day number 286 (January 13, 2020), the sensors were raised ~1 m from the bottom of the SC1 and SC2, and the water level below these sensor positions was not measured. Some of the gaps in the data in Fig. 14 also reflect these changes.

Table 1. The timeline for the data interruption

Date Start, Time	**Date End, Time**
04/09/2020, 14:00	04/11/2020, 20:45
06/05/2020, 10:07	06/29/2020, 6:58
08/21/2020,14:31	09/20/2020, 4:27
11/11/2020, 14:45	11/13/2020, 1:26
11/18/2020, 4:11	12/18/2020, 19:38
03/05/2021, 8:17	05/08/2021, 00:12

Fig. 15 shows the daily inflow of water for the 6th-10th day of monitoring. On day 6, the water level in SC1=0, DW1= 7.5 m, SC2=0, and DW2=3.5 m. This shows the presence of standing water in DW1 due to poor hydraulic performance and a perched water table in DW2 (Sasidharan et al., 2020). The overall data shows a very good daily cycle of filling up SC1, DW1, SC2, and DW2 and subsequent draining in a consistent pattern. Figs. 16 A and B shows one complete filling and draining cycle on Day 6. The water started to fill the SC1 at 9137 min, and when the SC1 water level reached approximately 1 m, the DW1 starts to fill at 9153 min. This behavior was not expected as the OVF1 in SC1 is at 2.8 m. This observation demonstrated that SC1 and DW1 act as a single chamber when the water reaches approximately 1 m in SC1, due to the leaking of water through the sidewall holes originally designed to aid the draining of any leftover ponded water from SC1 after a storm event. Once the water level reaches 21 m in DW1 at 9173 min, the slope changes, reflecting the filling of OVF1 from the bottom of DW1. When the water level reaches 3.6 m in SC1 and 23 m in DW1 at 2197 min, the water flows through the connection pipe into SC2. Interestingly, when the water level reaches 2 m in SC2 at 9215 min, the DW2 started to fill. Once again, this behavior was not expected as the OVF2 is at 3.7 m in SC2. Therefore, this behavior can be attributed to the leaking of water through the holes of the SC2 wall. The sidewall around SC2 is filled with gravels and pebbles, and directly connected to DW2, as shown in Fig. 13. Therefore, it is recommended that future designs should eliminate the perforated holes on the SC wall and develop other approaches to drain the SC at the end of a storm event.

Fig. 16 C shows the draining behavior for all four chambers. The SC1 has drained completely in 725 min, whereas SC2 has drained in less than 50 min. The DW2 has drained and reached the starting water level of approximately 4 m in 725 min. At the same time, the DW1 has only drained about 5 m and reached 18 m compared to the starting water level of 6.5 m after 725 min. Fig. 17 shows the long-term drainage behavior from Day 14 (a 0.13" rain event) to Day 26 of monitoring. This data shows that the DW1 has drained from 23 m to 3 m in 12 days and confirms the poor hydraulic performance of DW1 due to clogging. In contrast, the DW2 data shows no significant change in the perched water table level, and this is consistent with the observation of a thick clay layer at the bottom of the drywell that prevents the draining of this perched water. These observations will be discussed in detail in later sections. Fig. 18 shows the summer period of 2019 with no rain event. However, the daily water inflow showed a consistent filling and draining pattern in all the chambers. This daily inflow of water can contribute to constant head conditions at the site. Such conditions can enhance recharge but also faster migration of contaminants to groundwater (Sasidharan et al., 2020; Sasidharan et al., 2021).

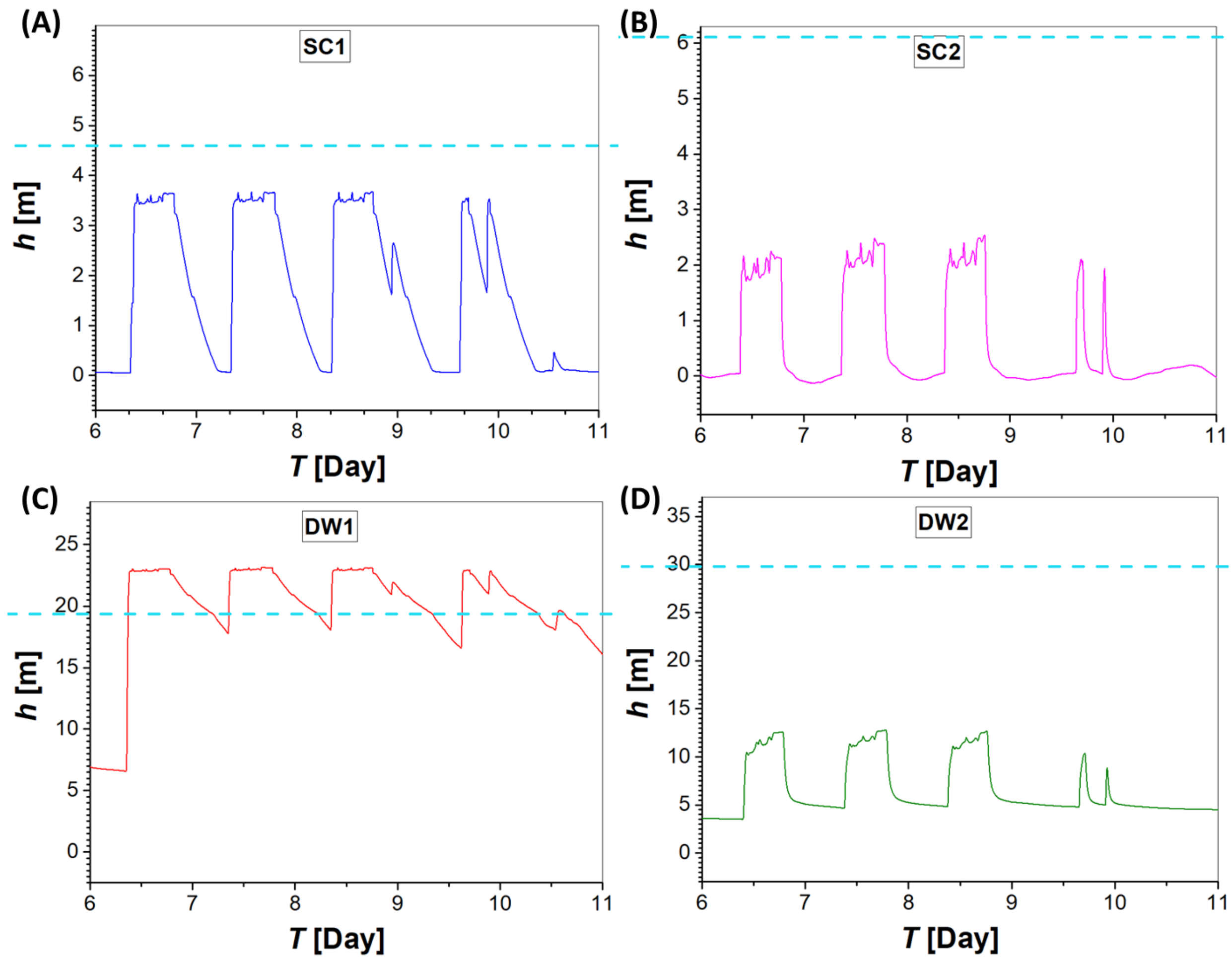

Figure 15. The daily inflow of water for five consecutive days, starting on Day 6 in SC1 **(A)**, SC2 **(B)**, DW1 **(C)**, and DW2 **(D)**.

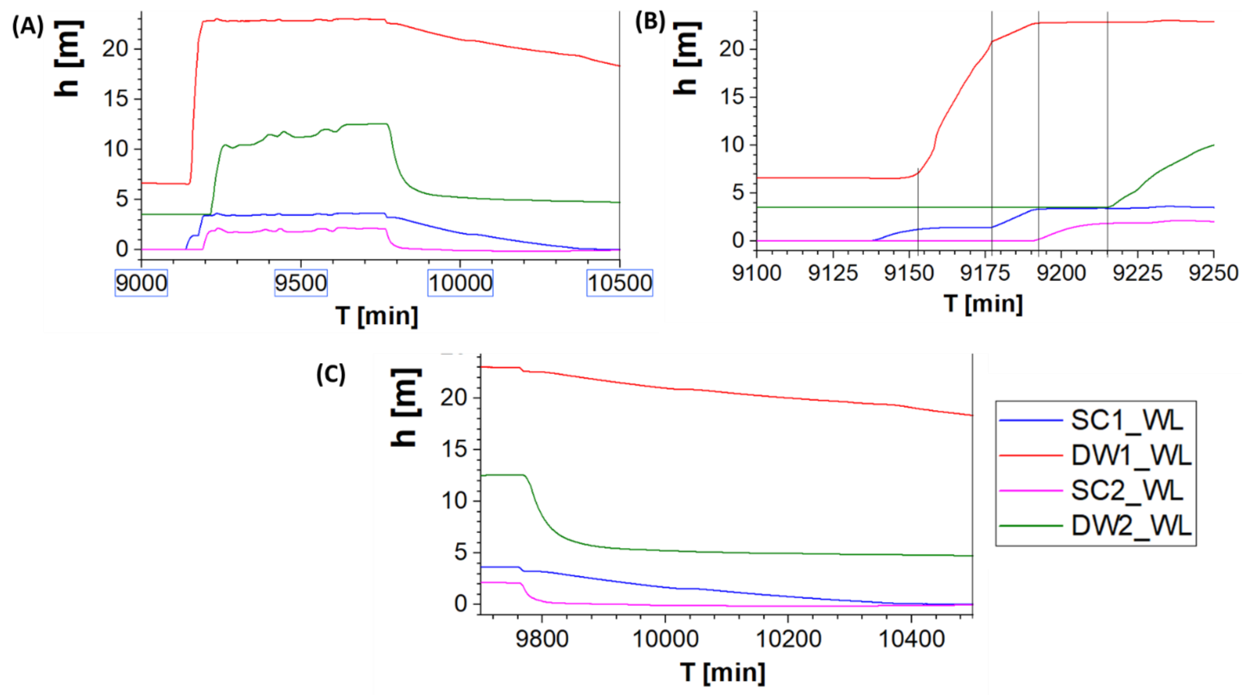

Figure 16. The daily water inflow and draining cycle for SC1, SC2, DW1, and DW2 for the 6th day **(A)**. The zoomed (time) analysis of water flow dynamics in all the chambers during inflow **(B)** and draining **(C)**.

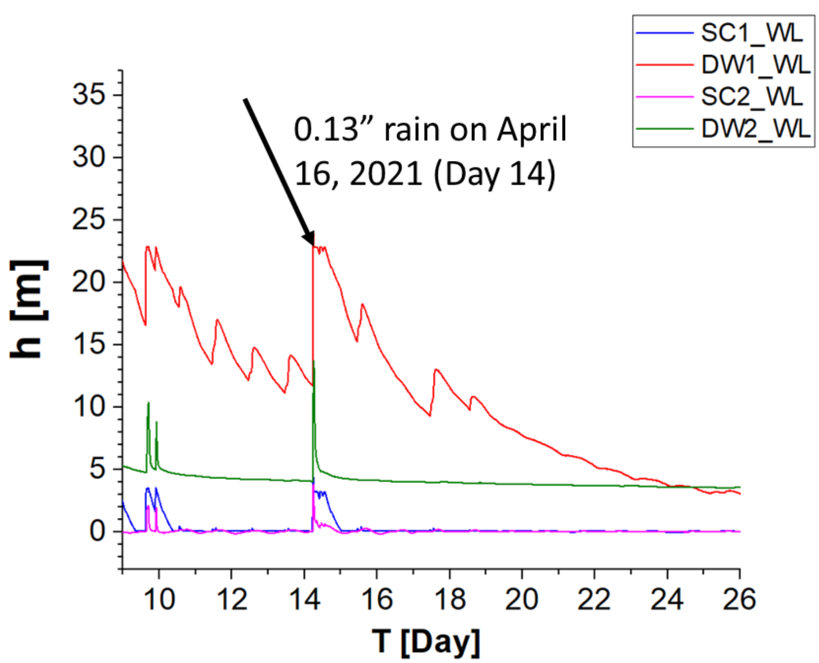

Figure 17. The daily water inflow during Day 9-Day 26 and 0.13" rain event on Day 14 (April 16, 2019).

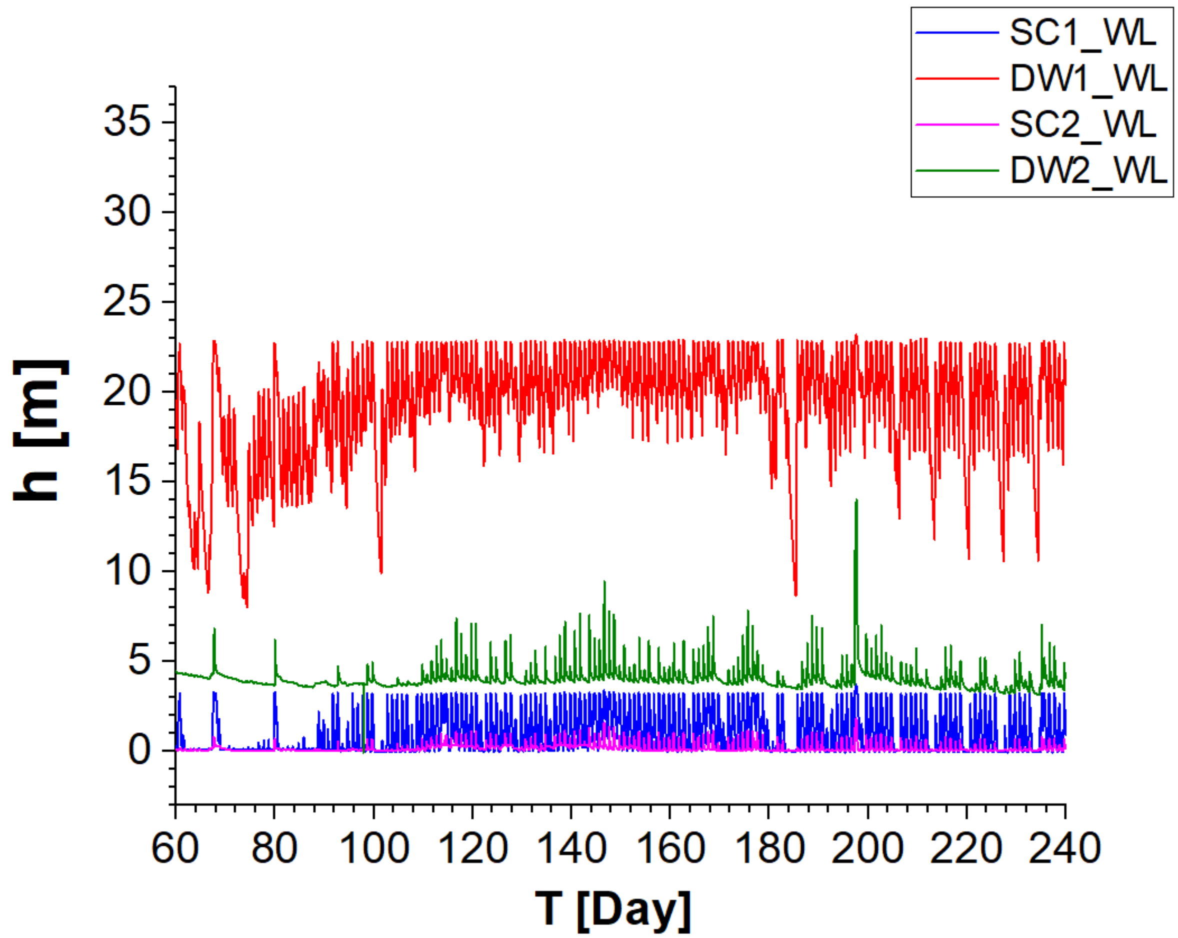

Figure 18. The daily water inflow cycle during Day 6 (06/01/2019)-Day 240 (11/28/2019) for summer 2019.

7.3. Hydraulic Performance of DW1

The hydraulic properties of the DW1 were determined using the falling head test in 2017 (Sasidharan et al., 2018). Further experiments were not conducted in a controlled manner. However, the frequent daily inflow and occasional rain events provided an opportunity to evaluate the performance of the drywell in more detail. Fig. 19A shows selected rain events and the water level height in DW1. Fig. 19B shows that the duration of all the rain events was different. Therefore, the start time was adjusted to correspond with a water level height of 16 m in plots shown in Fig. 19C and 19D. Interestingly, the data shows no change in the hydraulic performance of the well during these events. The falling head behavior changed throughout the monitoring period. The observed changes may be attributed to the difference in the initial condition of the soil around the well due to the frequency or duration of storm events, drying periods, or daily inflows. Therefore, the falling head behavior of DW1 was investigated for days where daily water inflow or a significant rain event was not present on that day, and the SC1 water level was zero. Fig.

20 presents the result for falling head from 18 m to 10 m in DW1. However, this data also does not show any specific pattern or decrease in infiltration rate, and the water level reached 10 m within 1500-2500 min. This result suggests that our frequent maintenance of DW1 (e.g., removing the sediments, protecting with rocks, and placing the mesh cover on OVF1) helped maintain its hydraulic performance since 2019.

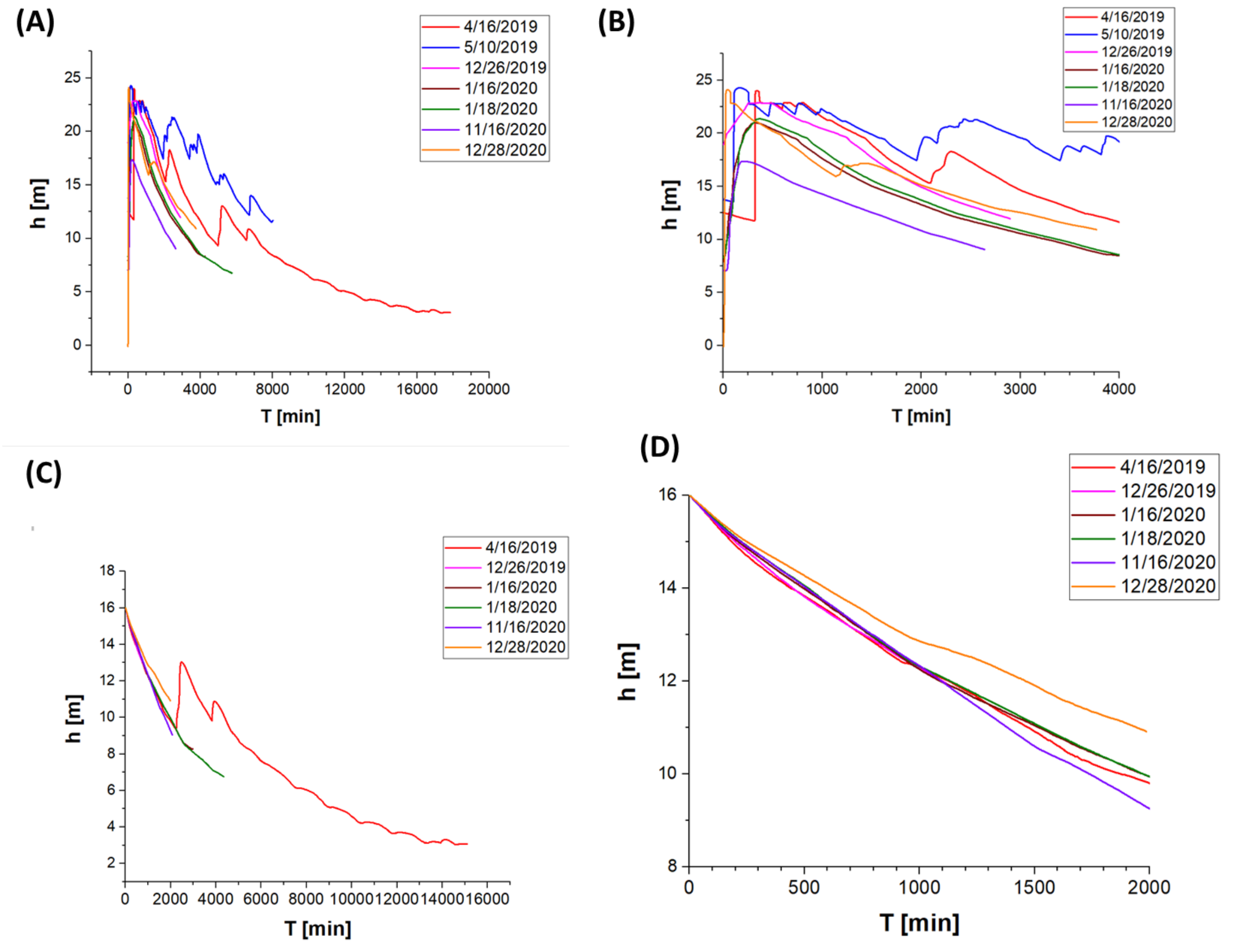

Figure 19. Selected rain events at the Fort Irwin site for DW1 **(A and B)** and data adjusted to show all the events starting at the water level of 16 m for DW1 **(C and D)**.

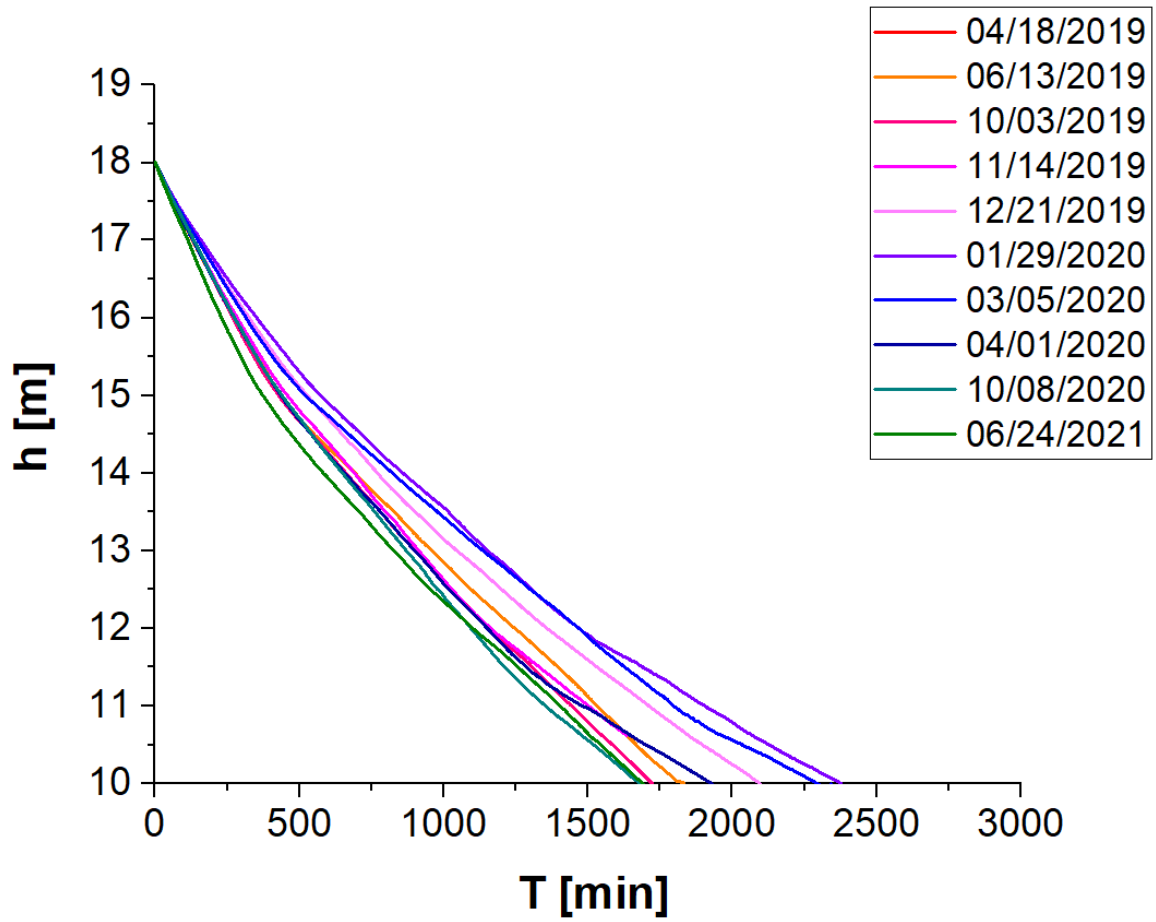

Figure 20. The draining of water level from 18 m – 10 m for the DW1 for a period where daily inflow or rain event was not present at selected dates over three years.

7.4. Hydraulic Performance of DW2

The hydraulic properties of DW2 were determined previously and explained in detail in (Sasidharan et al., 2020) (Chapter 4). Additional investigation was conducted using the storm event data from the last three years. Fig. 21 shows four selected rain events and the falling head behavior for DW2. Interestingly, the event on 12/28/2020 showed the fastest drainage compared to the previous events. However, this event was the smallest of all four events. Changes in the initial condition and the amount of water in the perched water table may explain these differences in drainage behavior. Additionally, data analysis was conducted by looking into the falling head behavior from 5 m to 4 m, when no daily inflow or rain event was present (Fig. 22). As seen in DW1, no specific pattern or reduction in hydraulic performance was observed during the monitoring period. Fig. 23 showed the falling head behavior when the water inflow frequency was the longest, and again no specific pattern was observed. Fig. 24A shows the water level in DW2, and Fig. 24B shows the lowest water level observed in DW2. This data shows that after 650 days of monitoring, the DW did not receive much daily water inflow or significant rain events. This interval corresponds to the drought period observed in California in 2020-2021 and probably changes in the scheduling and volume of irrigation water at Fort

Irwin. Overall, the hydraulic performance of DW2 did not significantly change during the monitoring period.

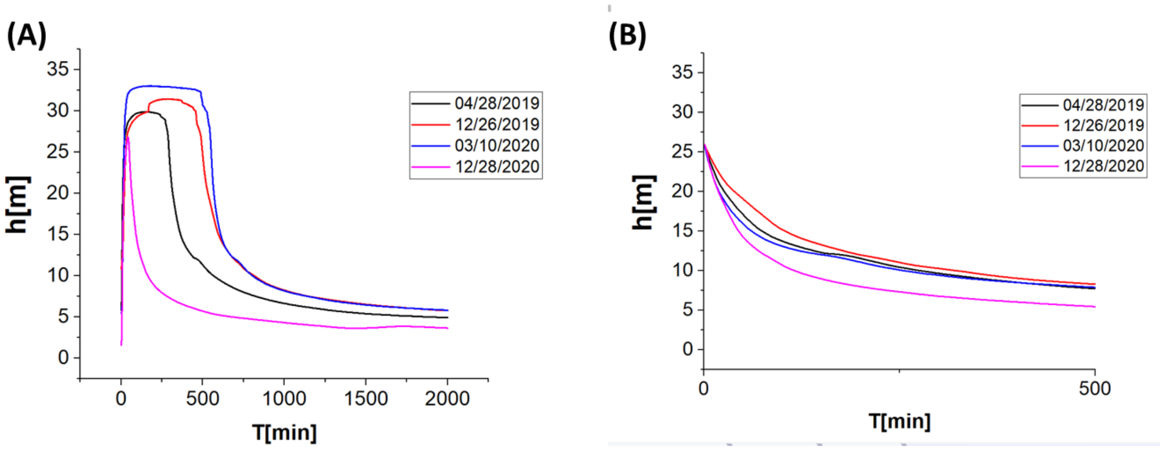

Figure 21. The falling head data from the DW2 during four selected rain events **(A)**. Data adjusted to show all the events starting at water level=25 m for DW1 at different x-axis and y-axis scale.

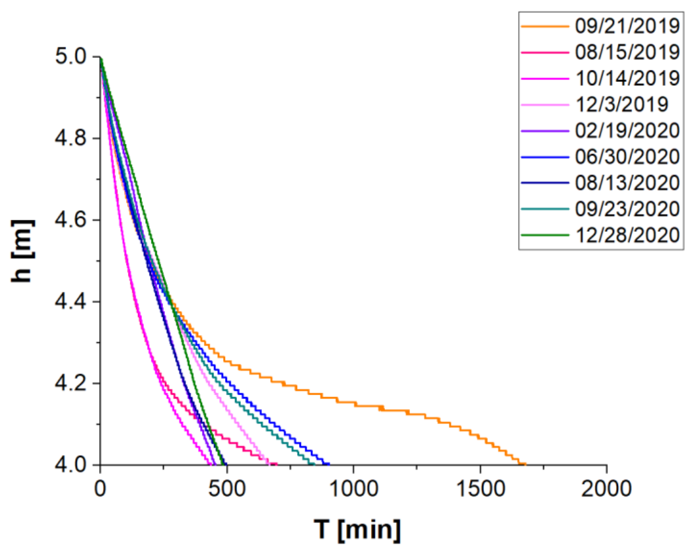

Figure 22. The drainage of water height level from 5 m – 4 m for the DW1 for a period where daily inflow or rain event was not present at selected dates over the three years.

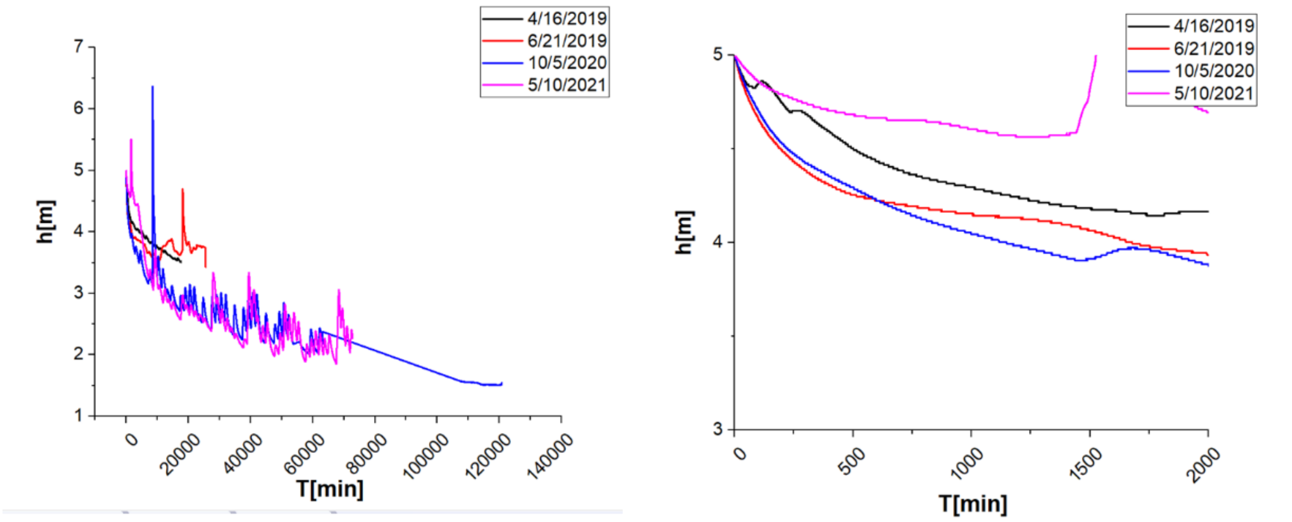

Figure 23. The falling head data for the perched water table from DW2 during four time periods when the water inflow frequency was the lowest. Note that there is a data gap in 63144 min-107273 min, where the data was not available.

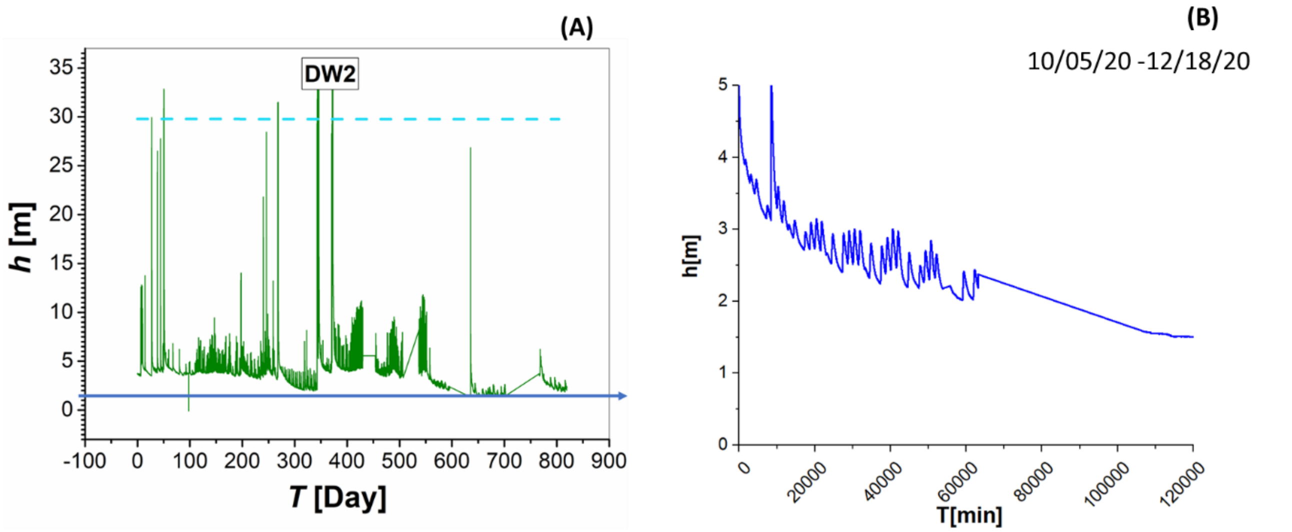

Figure 24. The water level data for DW2 **(A)** and the lowest water level observed in DW2 **(B).**

7.5. Turbidity in Drywells

Fig. 25 shows the change in turbidity in SC1 and SC2 during the daily inflow or rain events. These results show that both SC1 and SC2 received a significant amount of clay during the monitoring period. However, the turbidity collected every minute and the cumulative amount of clay received in an individual event is challenging to calculate because the incoming water flow stirs up sediments in the bottom of the SC. In addition, some sediments escaped through the overflow pipe into the lower chambers. Therefore, the overall turbidity data shows that a sedimentation chamber alone may not help prevent the accumulation of sediments into the lower chambers. Additional pretreatment is necessary to eliminate the sediments, thus preventing clogging and expanding the life span of the drywell.

.

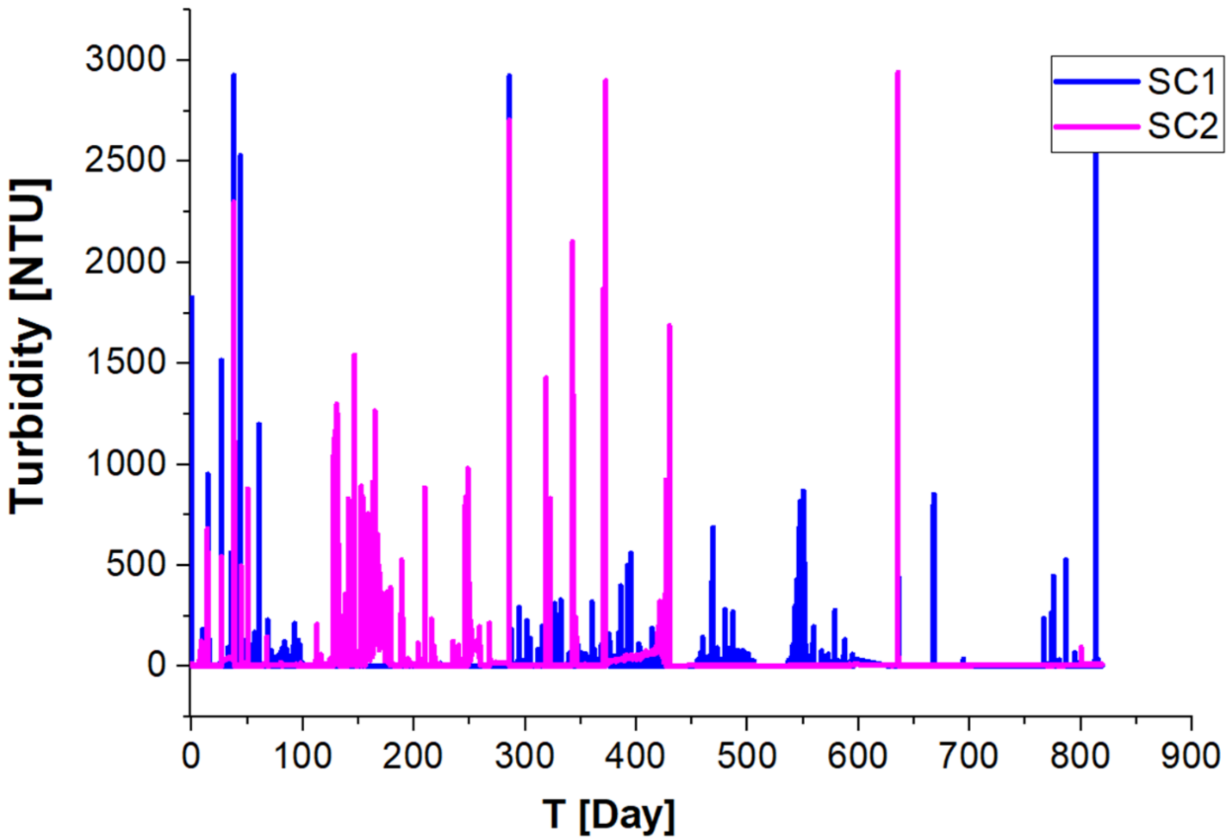

Figure 25. The measured turbidity changes during daily inflow or rain events in sedimentation chamber 1 (SC1) and sedimentation chamber 2 (SC2) from 04/12/2019-06/29/2021.

7.6. Perched Water Table – Slow Response to Infiltration Events

Fig. 26 shows the perched water table level (at 37.4 m) in the MW from Dec 2019 through June 2021. The result shows that the perched water table receives water on major rain events and during daily inflows.

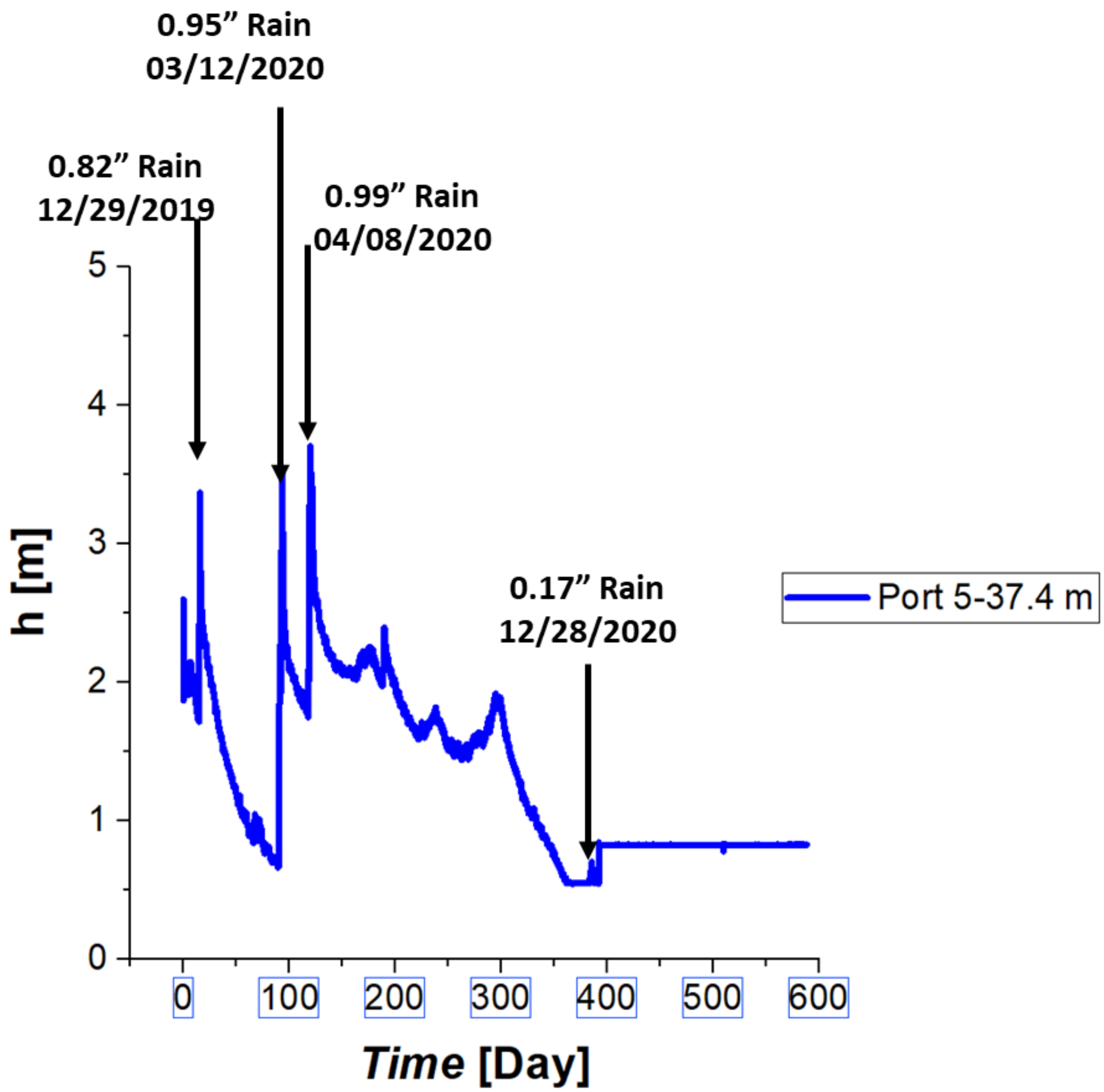

Figure 26. The water level measurement from the perched water table was observed at the monitoring well. The water level response associated with rain events is highlighted in the figure.

7.7. Monitoring Well – Response of Perched Water Table to Recharge Events

Figure 27 shows the lowest observed perched water table level in the monitoring well. The data shows that by around 380 days since monitoring (1/1/2021), the water level has reached approximately 0.5 m (Fig. 27A) and remained at that level until day 400. Note that the sudden increase in water level from ~0.5 to 0.83 m (Fig. 27A and 27B) is due to the change in position of the water level sensor within the well (Fig. 27C). Every couple of months, USGS collects water samples from the monitoring well for groundwater analysis (corresponds to a site visit on 01/06/2021). During this time, the sensors are retrieved and placed back, and a slight change in elevation of the water level sensor may happen, which is reflected as shown in Fig. 27A and 27C. Interestingly, the water level is constant at ~0.83 for the past 200 days. This data shows that once the water level reaches ~0.83 m, the infiltration rate of the perched water table is extremely low. The slight anomaly on day 509 shows a site visit by UC Riverside on 05/04/2021, and the sensors were secured and marked with the correct height to maintain the elevation during future site visits.

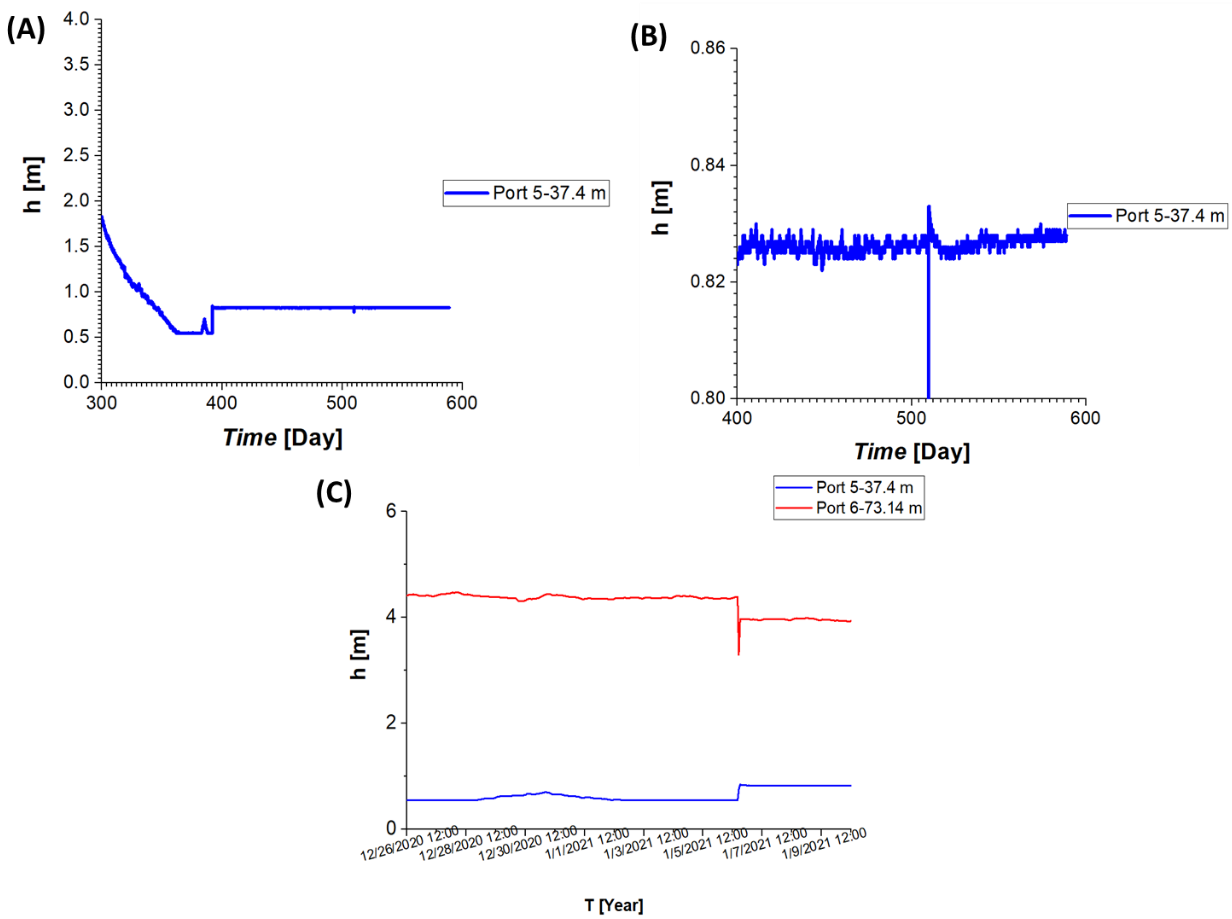

Figure 27. The lowest water level observed for the perched water table in MW **(A)**, daily fluctuations in day 400 to 600 **(B)**, the water level in the perched water table (blue), and the groundwater (red).

7.8. Water Content Sensors Above and Below Perching Layer

Fig. 28 shows the water content measurement in the MW using TEROS 12 (Meter group) sensors at four depths, i.e., 1.52 m and 27.4 m (placed above the clay layer), and 41.5 and 48.8 m (placed below the clay layer or perched water table). The data shows some change in water content at Port 1=15.2 m during the early 2020 rain events. However, no significant changes were observed since April 2020. In contrast, Port 2=27.4 m shows a value of 0.55 consistently. The soil at the DW site is sandy clay loam in texture, and a value of 55% VWC is not expected. However, Fig. 28C shows that the saturation

Extract Electrical Conductivity changes over time. Many of these changes are not directly correlated to any known field events. For example, the value of EC increased from 6.723 to 13.626 on 11/17/2020 3:00:00 PM. According to Meter Group, the sensor in port 2 has an enormous bulk electrical conductivity, and that is why its volumetric water content is maxed and not changing. An EC that high will interfere with the VWC reading. The only way to explain such a high EC is the presence of a very high concentrated salt pocket at this location. However, the presence of such a high salt pocket at this site is not expected, and, therefore, such observations are unexplainable. Figs. 28A and 28C show that Port 3=41.5 m has a constant value throughout the monitoring period and demonstrates that the water from the perched water table is not reaching below the clay layer. Figs. 28A and 28C show that the sensor at Port 4=48.8 m stopped working after 200 days of monitoring. Several attempts were made to retrieve the sensor function by unplugging and resetting, but this failed to work. Fig. 28B shows the temperature data at four depths collected from the TEROS 12 sensor. A reasonable trend is seen with elevated temperature in the summer months and a decline in temperature during the winter months. The data also showed daily temperature changes. However, observed changes in temperature did not correlate with any specific pattern (day and night) or daily inflow of water (midnight to morning) at the site (Fig. 29, Summer 2020).

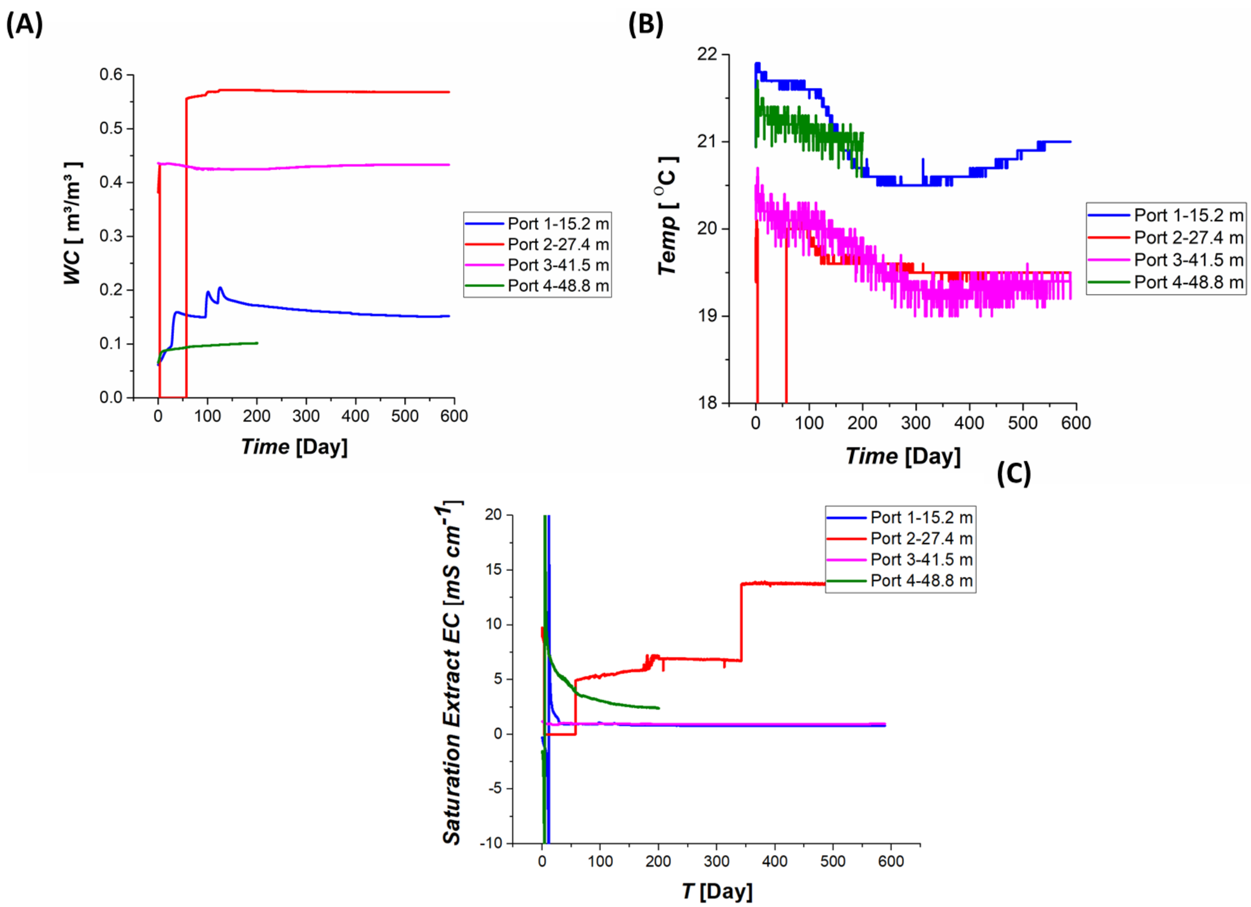

Figure 28. The water content **(A)** and temperature **(B),** and saturated extract EC **(C)** measured at four depths at the vadose zone monitoring well.

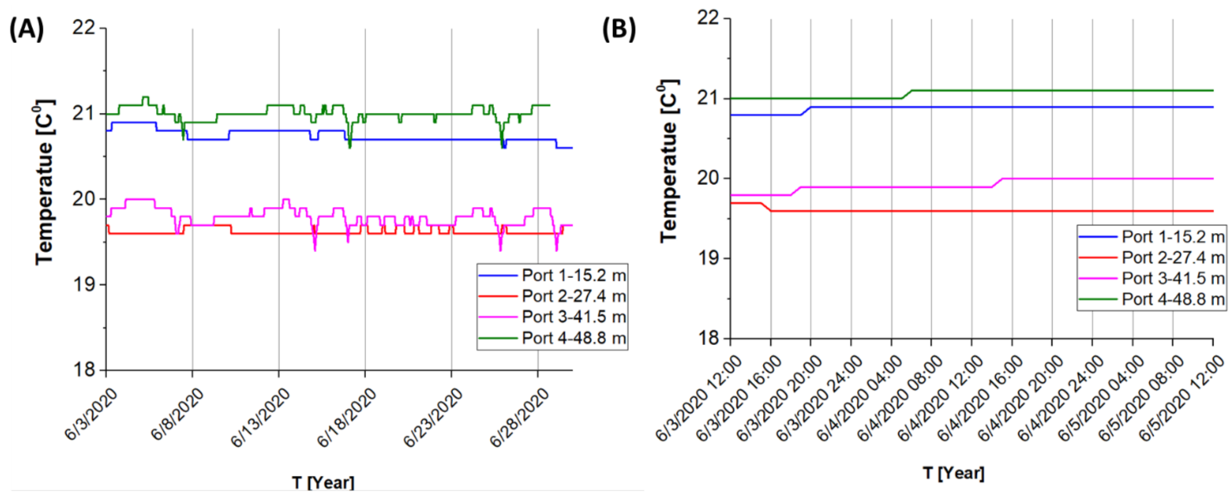

Figure 29. The measured daily temperature at four depths in the vadose zone monitoring well during June 2020 **(A)** and representative data for one day and night **(B)**.

7.9. Groundwater Level Changes

Fig. 30 shows the observed water level at the groundwater table at Fort Irwin. The water level ranged between approximately 3.5 m to 4.5 m. However, these observed jumps in the data (56, 207, 312, and 391st days) were due to the elevation change in the water level sensor when USGS collected the water sample from the monitoring well and removed the sensor, and reinstalled it back in the well. Fig. 31 shows the water level data where the observed data is corrected for the elevation changes before and after the reinstallation of the sensor. The data shows that the water level remained at an average value of 4.4 m throughout the monitoring period. Fig. 32A shows the measured water level between days 30-50, and Fig. 32B shows the water level between days 30-34. Fig. 32 shows the daily changes in water level at the site where the water level drops up to 20 cm and raises back to the original water level. This can be attributed to the changes in atmospheric pressure. Fig. 33 shows the effect of pumping in the water level at the site. The water level dropped from an average highest value of 4.6 m in the winter to an average lowest value of 4.2 m in summer. Therefore, the groundwater table has a 0.436 m decline annually due to the excessive pumping in the summer period, and the water level rises back to the pre-winter value when pumping rates go down in winter. Any contribution of recharge into the groundwater table during the winter months is not known at this time. This data demonstrates that the considerable variability in groundwater level on a daily scale at a meter-scale will prevent the determination of any recharge at the water table. Sasidharan et al. 2020 demonstrated that the subsurface heterogeneity could influence the arrival time and location of recharge water at the water table. Therefore, additional techniques such as tracers and chemical signatures are essential to accurately determine the recharge from many MAR schemes.

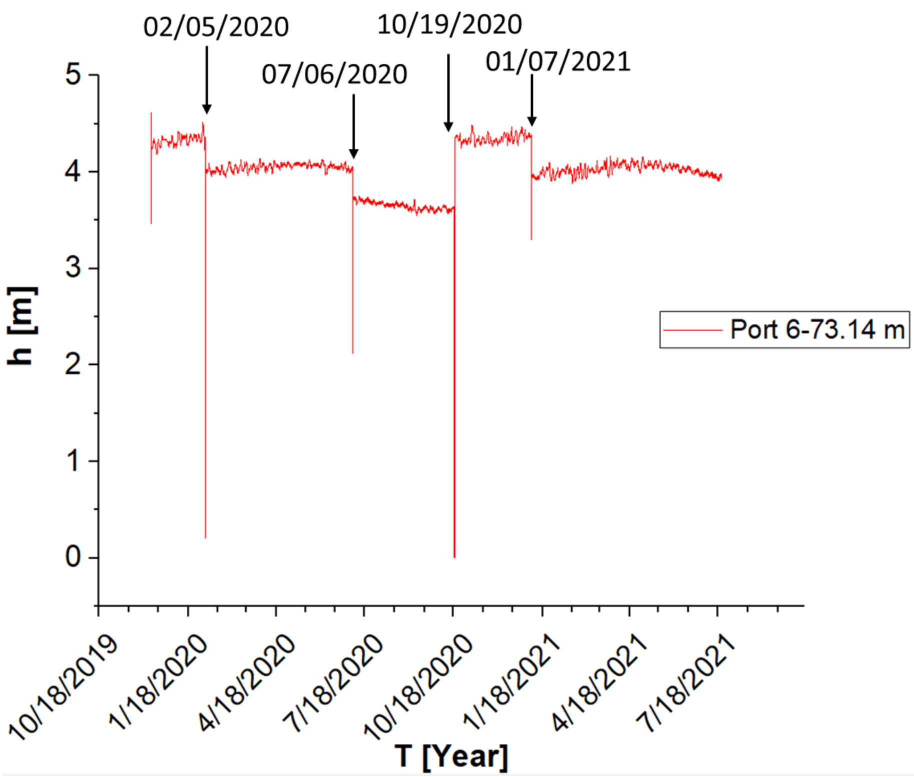

Figure 30. The measured water level for the groundwater table at Fort Irwin during December 2019-June 2021. The highlighted dates show the activities in the MW, such as water sample collection or water level measurement.

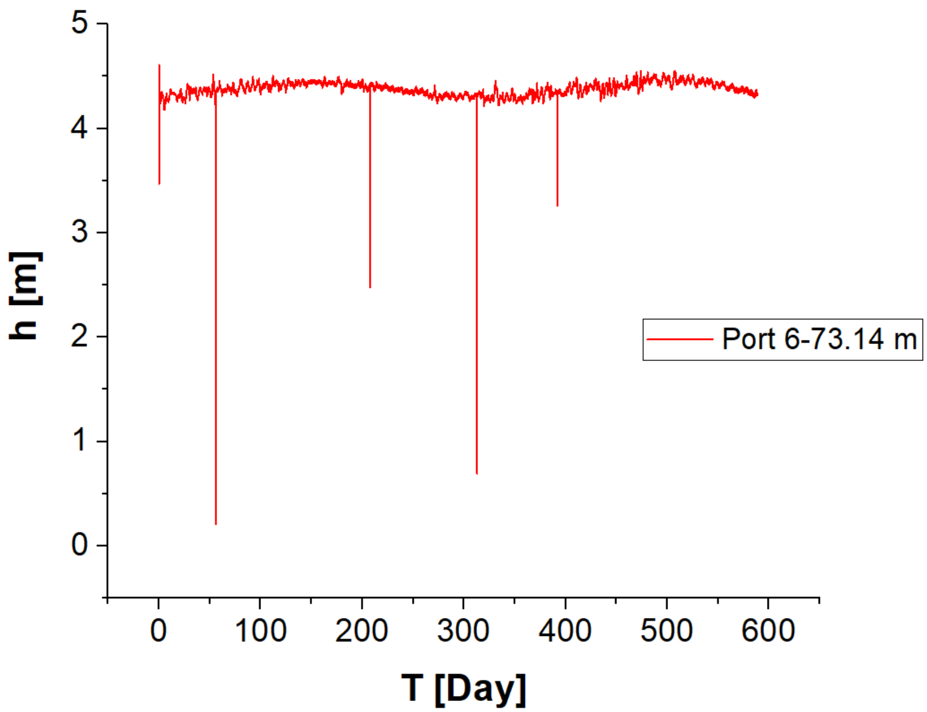

Figure 31. The measured water level for the groundwater table at Fort Irwin during December 2019-June 2021. The water level is adjusted to the day one measurement by considering the changes during water sample collection days.

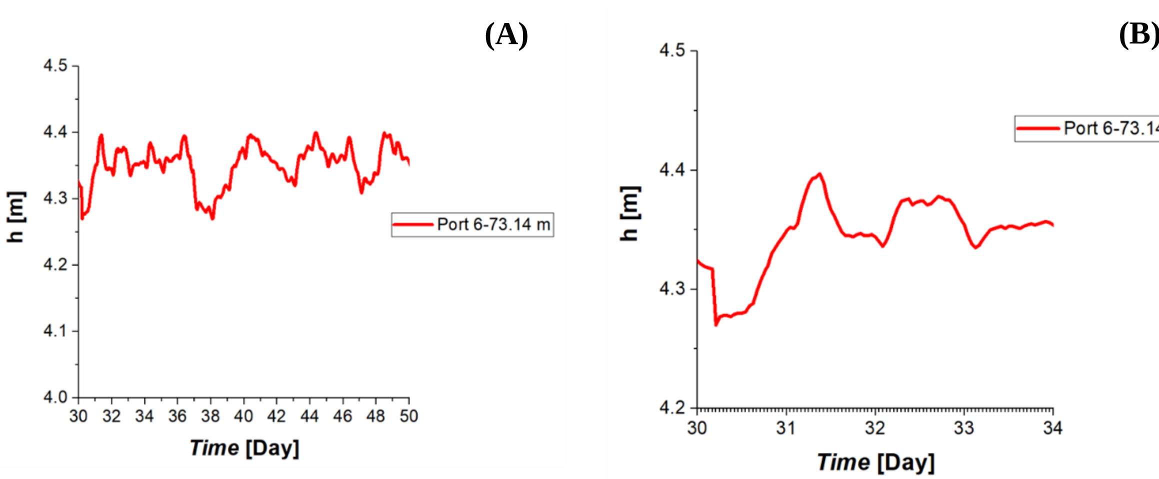

Figure 32. The measured water level for the groundwater table at Fort Irwin during Day 30th-50th **(A)** and Day 30th-34th **(B).**

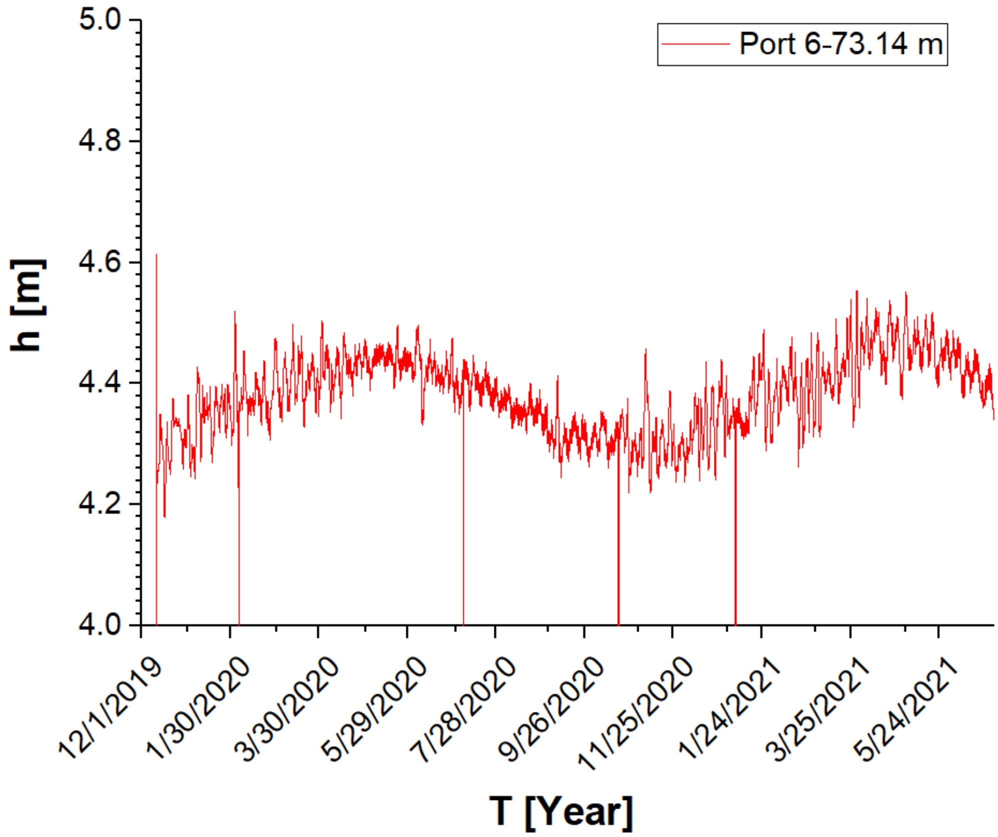

Figure 33. The measured water level for the groundwater table at Fort Irwin during December 2019-June 2021 shows the pumping effect in the summer and winter.

7.10. The Fort Irwin Basin Performance-March 2020 Storm Event

The previous sections explored the overall performance of the drywell, the water flow dynamics, and its response in the perched water table and groundwater table. This section will explore the complete basin, DW, perched water table, and groundwater responses to a storm event. In March 2020, the site received an average of 1.86" rain, with 0.75" rain on 03/10/2020, 0.04" rain on 03/11/2020, and 0.95" rain on 03/12/2020 (Fig. 34). Fig. 35 shows the drainage of the basin after the March 13 event, where the data was collected from a site camera. Note that the camera turns off at night or when the cloud coverage is high, and therefore, only a few specific images were collected. As shown in this figure, the basin was drained entirely within 24 hours. Fig. 36 shows the water level in SC1, DW1, SC2, and DW2 during 03/06/2020-03/18/2020, and Fig. 37A shows the same data where starting time is adjusted for this specific period.

Fig. 37B shows the filling cycle for the rain event on 03/13/2020. Before the rain event, the DW1 has 13 m of water, and at the beginning of the rain event, the DW1 fills up first (~6739 min) instead of SC1, since both SC1 and DW1 are connected through the sidewall holes, as explained in the previous section. Note that the sensors are placed 1 m above the SC1 bottom, and therefore, the water level will be only captured at >1 m.

The SC1 and DW1 filled up to the connection pipe within 10 min (at ~6748 min), and the water started to fill SC2. When the water reaches approximately 3 m, the DW2 started to fill. The water might have reached the DW2 initially through the sidewall hole, but as the SC2 filled up, the water went into DW2 through the overflow pipe in oppose to the SC1 and DW1. This behavior shows that the leaking of SC2 into DW2 is slower than the SC1 to DW1. However, this behavior was not expected in the original drywall engineering design. The presented data confirm that the sidewall holes can lead to leaking from SC, potentially escaping sediments into the lower chamber, and subsequent clogging. At 6,840 min, the SC1 and DW 1 were filled, and the basin had approximately 1.6 m of water. Note that both SC2 and DW2 never went above their maximum capacity of 6.1 m and 35.9 m and confirms that the DW2 is not connected to the basin directly as designed by Torrent Resources, and the entire system act as a MaxWell Plus system at the site. Fig. 37C shows the draining behavior of all four chambers. At around 8200 min, the water level in SC1 and DW1 reached below the connection pipe, and the DW2 and SC2 started to drain immediately. The SC2 was drained entirely in less than 50 min, and the water level in DW2 reached ~6 m within 3,200 min.

Fig. 37C shows that at ~8,500 min, the site received another small event, and both DW1 and SC1 was filled, and the water entered the SC2 and DW2 through the connection pipe. The water level in SC1 and DW1 was maintained at the connection pipe level from 8,500-8,900 min. However, note that the SC2 does not show any water level because the water level sensors are placed 1 m above the SC2 bottom surface, and therefore, water level below 1 m will not be recorded. At 10,200 min, the DW1 shows another inflow of water (daily flow) and shows no change in water level in SC1, SC2, and DW2. This data confirms that DW2 only receives water from SC1 through the connection pipe to the SC2 and then to DW2 by leaking on the sidewall or through the overflow pipe.

Fig. 37D shows the corresponding value of turbidity in SC1 and SC2. The turbidity value in SC2 is higher than SC1. This is due to mixing all the sediment from the bottom of the SC2 during the initial rain event. Whereas SC1 receives water every day, and the sediments might be washed out to the DW1 or the SC2. Interestingly, after the first storm event (3,000-5,000 min), the turbidity level in SC1 and SC2 went very low. These results demonstrate that all the sediments in SC2 were washed out into the DW2, and the sedimentation chamber is not a great mechanism to accumulate the clay particle for the longer term. A major rain event can stir up these sediments, release them into the lower chamber, and eventually clog the system. Therefore, additional pretreatment mechanisms are necessary to capture these sediments effectively.

Fig. 38A shows the water level in the perched water table and the groundwater table. The perched water table increased approximately 1.5 m during the 03/12/2020 rain event, whereas the groundwater table did not show any change in water level. Fig. 38B shows the temperature of both the perched water table and the groundwater table. The temperature in the perched water table has decreased ~0.5°C due to the incoming cold water from the storm event. Fig. 39A shows the water content data above and below the perched water table. The WC sensor at Port 1= 15.4 m shows a slight increase in water content, demonstrating the infiltration from the basin as wells as drywells. However, all three other sensors did not show any change in water content. Ports 2 and 3 are at a constant value due to unexplainable reasons, and Port 4 did not show any water content change confirming that the perched water table is not draining at this location. However, the decrease in water level in the perched water table (Fig. 38. A) confirms that the perched water table is draining; the extension of the clay layer and the location of the bypass are unknown from currently available data. Fig. 39B shows the temperature at four depths in the vadose zone. Interestingly, Port 1 did not show any temperature change. However, all other three sensors had some variabilities. The exact mechanism for these observed temperature changes is unclear; however, it might be correlated to changing atmospheric temperature in day and night or cold/warm days, or variations in earth's thermal energy.

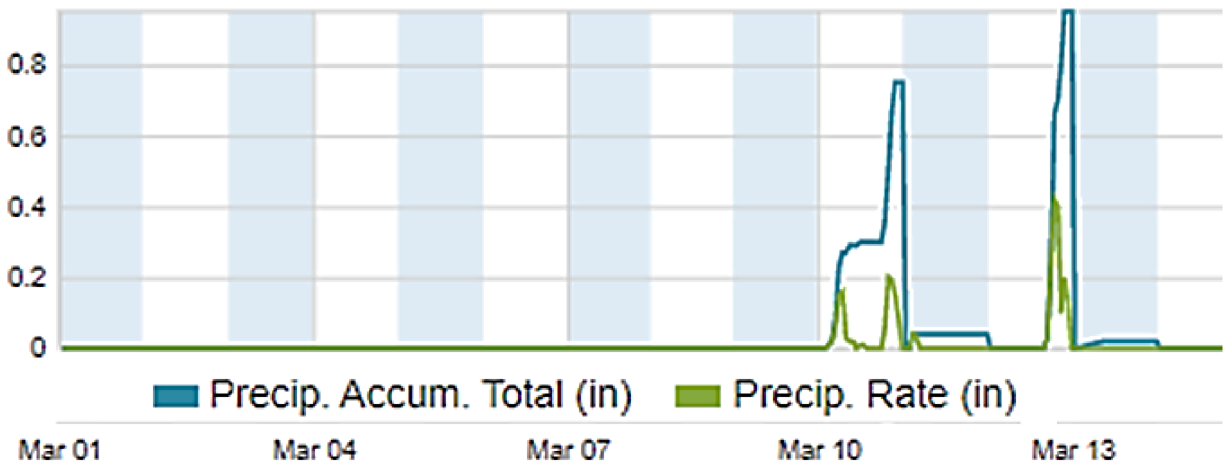

Figure. 34. The precipitation at Fort Irwin on March 10 – 13th, 2020.

Figure 35. The time-lapse images of the basin draining after the March 12, 2021, storm event.

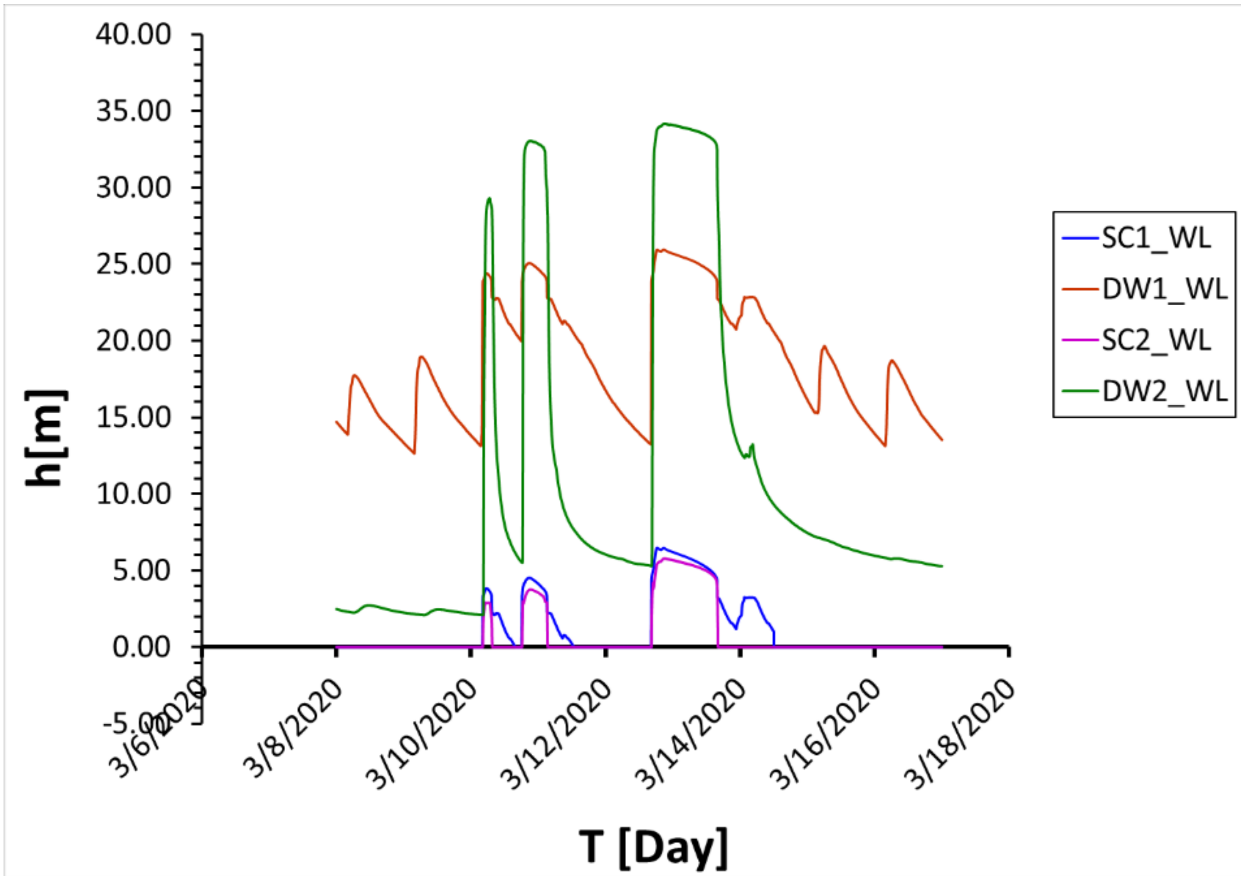

Figure 36. The water level data observed in SC1, DW1, SC2, and DW2 between 03/06/2020-03/18/2020.

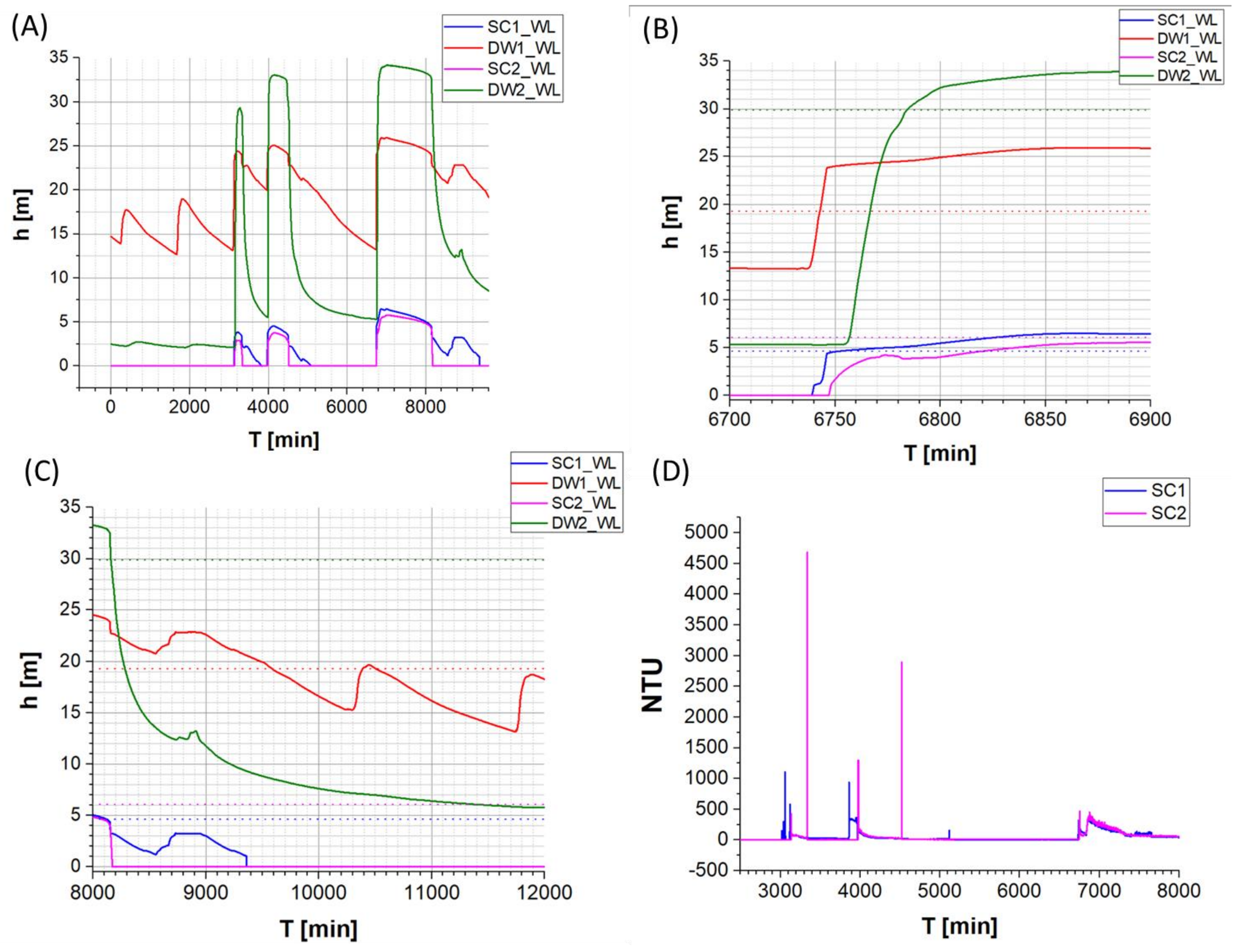

Figure 37. The water level in SC1, DW1, SC2, and DW2 adjusted to time **(A)**, the filling **(B)** and draining **(C)** behavior in all the chambers for the storm event on 03/12/2021. The corresponding turbidity value in SC1 and SC2 **(D).**

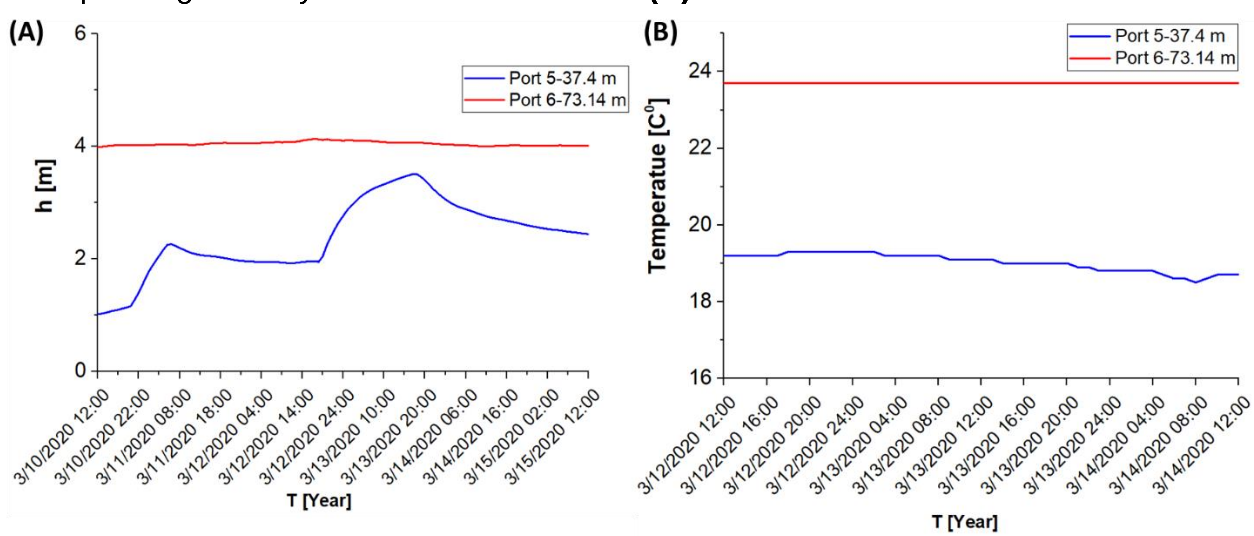

Figure 38. The water level **(A)** and temperature **(B)** in the perched water table (Port 5) and groundwater table (Port 6) for the storm event on 03/12/2021.

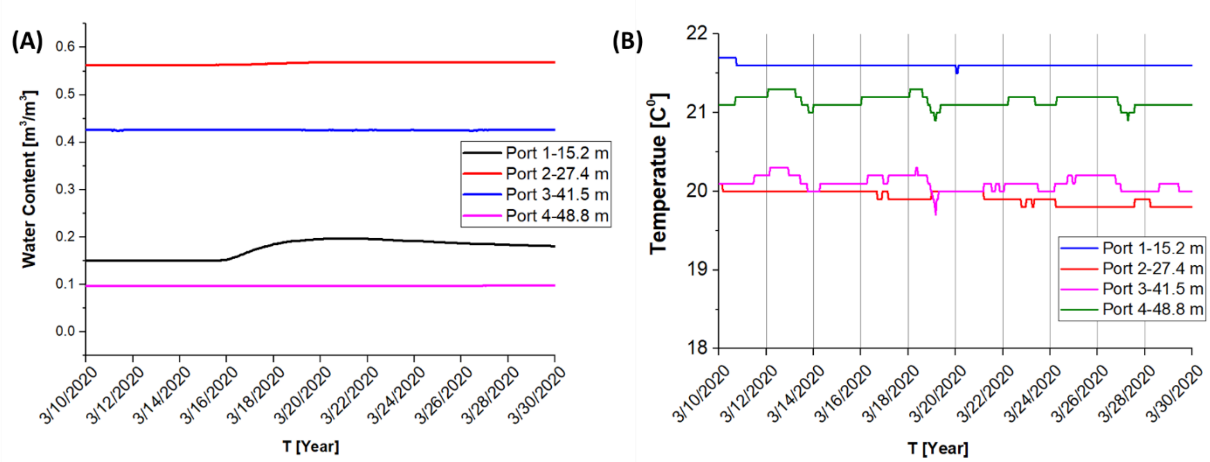

Figure 39. The water content **(A)** and temperature **(B)** at four depths in the vadose zone during 03/10/2020-03/30/2020.

8. KEY FINDINGS

Summary

Many arid and semiarid regions worldwide face challenges in maintaining water quantity and quality needs for growing populations. A drywell (DW) is an engineered vadose zone infiltration device widely used for stormwater capture and managed aquifer recharge, but only limited research has quantitatively determined the performance of DWs. Therefore, numerical and field-scale experiments were conducted to improve our understanding and ability to characterize the DW behavior. In particular, HYDRUS (2D/3D) was modified to simulate transient head boundary conditions for the complex geometry of the Maxwell Type IV DW, i.e., a sediment chamber, an overflow pipe, and the variable geometry and storage of the DW system with depth. Falling-head infiltration experiments were conducted on DWs located at the National Training Center in Fort Irwin, California (CA) and a commercial complex in Torrance, CA, to determine in situ soil hydraulic properties (the saturated hydraulic conductivity, Ks, and the retention curve shape parameter, α) for an equivalent uniform soil profile by inverse parameter optimization. A good agreement between the observed and simulated water heights in wells was obtained for both sites as indicated by the coefficient of determination 0.95-0.99–%, unique parameter fits, and small standard errors. Fort Irwin and Torrance DWs had very distinctive soil hydraulic characteristics due to the difference in site soil texture.

Studies were conducted to examine the role of ubiquitous subsurface heterogeneity in hydraulic properties on DW performance. Numerical experiments were conducted to systematically study the influence of subsurface heterogeneity on DW infiltration. Subsurface heterogeneity was described deterministically by defining soil layers or lenses, or by generating stochastic realizations of soil hydraulic properties with selected variance (σ) and horizontal (X) and vertical (Z) correlation lengths. The infiltration rate increased when a high permeability layer/lens was located at the bottom of the DW and had larger vertical and especially horizontal dimensions. Furthermore, the average cumulative infiltration (*I*) for 100 stochastic realizations of a given subsurface heterogeneity increased with σ and X, but decreased with Z. This indicates that the presence of many highly permeable, laterally extending lenses provides a larger surface area for enhanced infiltration than the presence of isolated, highly permeable lenses. This research provides valuable insight on the selection of site, design, installation, and long-term performance of a DW.

DWs are widely used as an infiltration device, but little research has examined the role of subsurface heterogeneity in hydraulic properties on DW recharge efficiency. Numerical experiments were conducted to systematically study the influence of various homogenous soil types and subsurface heterogeneity on recharge from DWs under constant head conditions. The mean cumulative infiltration (μI) and recharge (μR) volumes increased with an increase in the saturated hydraulic conductivity (*Ks*) for various homogeneous soils. For heterogeneous domain, after 365 days, values of μI, μR, and the radius of the recharge area increased with σ and X but decreased with Z. The

value of *μR* was always smaller for a homogeneous than a heterogeneous domain. This indicates that recharge for a heterogeneous profile cannot be estimated with an equivalent homogeneous profile. The value of *μR* was always smaller than *μI,* and correlations were highly non-linear due to vadose zone storage. Therefore, knowledge of only infiltration volume can lead to misinterpretation of recharge efficiency, especially at earlier times. The arrival time of the wetting front at the bottom boundary (60 m) ranged from 21 to 317 days, with earlier times occurring for increasing σ and Z. The corresponding first arrival location can be 0.1–44 m away from the bottom releasing point of a DW in the horizontal direction, with greater distances occurring for increasing σ and X. This knowledge is essential to accurately assess DW recharged performance, water quantity, and water quality.

No prior studies have quantitatively examined virus transport from a DW, especially in the presence of subsurface heterogeneity. Axisymmetric numerical experiments were conducted to systematically study virus fate from a DW for various virus removal and subsurface heterogeneity scenarios under steady-state flow conditions from a constant head reservoir. Low levels of virus concentration tailing can occur even at a separation distance of 22 m from the bottom of the DW, and 6-log 10 virus removal was not achieved when a small detachment rate (k_{d1} = 1 × 10 $^{-5}$ min^{-1}) is present in a homogeneous domain. Improved virus removal was achieved at a depth of 22 m in the presence of horizontal lenses (e.g., X= 10 m, Z= 0.1 m, σ= 1) that enhanced the lateral movement and distribution of the virus. In contrast, faster downward movement of the virus with an early arrival time at a depth of 22 m occurred when considering a vertical correlation in permeability (X= 1 m, Z= 2 m, σ= 1). Therefore, the general assumption of a 1.5–12 m separation distance to protect water quality may not be adequate in some instances, and site-specific microbial risk assessment is essential to minimize risk. Microbial water quality can potentially be improved by using an in-situ soil treatment with iron oxides to increase irreversible attachment and solid-phase inactivation.

DWs and infiltration basins (IBs) are widely used as MAR devices to capture stormwater runoff and recharge groundwater. However, no published research has compared the performance of these two engineered systems under shared conditions. Numerical experiments were conducted to systematically study the performance of a circular IB design (diameter and area) and partially penetrating DW (38 m length with water table > 60 m). The effects of subsurface heterogeneity on infiltration, recharge, and storage from the DW and IB under constant head conditions were investigated. The value of *μI* and recharge *μR* increased, and the arrival time of recharge decreased with the IB area. Values of *μI* were higher for a 70 m diameter IB than an DW, whereas the value of *μR* was higher for a DW after 1-year of a constant head simulation under selected subsurface heterogeneity conditions. A comparison between mean *μI*, *μR*, and mean vadose zone storage (*μS*) values for all DW and IB stochastic simulations (70 for each MAR scenario) under steady-state conditions demonstrated that five DWs can replace a 70 m diameter IB to achieve significantly higher infiltration and recharge over 20 years of operation. Additional numerical experiments were conducted to study the influence of a shallow clay layer by considering an IB, DW, and a DW integrated into an IB. The presence of such a low permeable layer delayed groundwater recharge from an IB. In contrast, a DW can penetrate tight clay layers, release water below them, and facilitate rapid infiltration and recharge. The potential benefits of a DW compared to an IB include a smaller footprint, the potential for pretreatments to remove contaminants, less evaporation, less mobilization of in-situ contaminants, and potentially lower maintenance costs. Besides, this study demonstrates that combining both IB and DW helps to get the best out of both MAR techniques.

The site-specific monitoring data from the Fort Irwin site gave detailed insight into the overall performance of the catchment, two drywells, connection pipes, and monitoring well installed at the Fort Irwin, CA site. The daily irrigation water input demonstrated that the drywells fill up and drain consistently, and a nearly constant head condition was maintained at the site. The drywells received a significant amount of clay from daily inflow and major storm events, and some of these sediments escaped into the lower chamber through the overflow pipe or the holes on the sedimentation chamber sidewalls. The infiltration rate from the old drywell is prolonged due to the clogging. The new drywell infiltrated water very fast, and the hydraulic conductivity has not changed much since installation. The perched water table level measured at the monitoring well responds to major rain events; however, no distinguishable changes in water level were observed during the daily inflow of water. The water content sensors above the perched water table respond to the rain event events; however, changes in water moisture contents were not recorded for water content sensors below the perched water table. The groundwater monitoring data show significant changes in daily response to the pumping activity. Therefore, monitoring any recharge using water level alone will not be possible, and new chemical signature methods need to be included for exclusive groundwater recharge monitoring.

Highlights

Chapter 2

- Falling-head infiltration experiments were conducted on two drywells located in California.
- HYDRUS (2D/3D) was modified with a new Reservoir Boundary Condition that accounts for the drywell's complex geometry.
- Effective soil hydraulic properties were estimated via inverse optimization of the falling head data.
- A highly permeable lens at the bottom of a drywell can infiltrate water at a much faster rate.

Chapter 3

- Cumulative infiltration volume increased with variance and lateral correlation length.
- Cumulative infiltration volume decreased with an increasing vertical correlation length.

- The average value of hydraulic conductivity played a primary role on drywell cumulative infiltration.
- Constant head experiments provide higher accuracy in inversely optimized hydraulic parameters.

Chapter 4
- Recharge volume for a homogeneous domain is smaller than a heterogeneous domain.
- Correlation between drywell infiltration and recharge volumes is highly non-linear.
- Cumulative recharge volume increased with lateral correlation length.
- Arrival time and location increase with a lateral correlation length
- Arrival time decreases with the standard deviation permeability and the vertical correlation length.

Chapter 5
- A 1.5–13 m separation distance is inadequate for virus removal in many instances.
- Virus concentration tailing occurs due to low detachment and sticking efficiency.
- Virus transport can be mitigated by increasing irreversible attachment and solid phase inactivation.
- Virus transport is greater for high hydraulic conductivity and vertically extended permeability.
- Horizontal permeability promotes lateral distribution and removal of viruses.

Chapter 6
- Infiltration and recharge increase with the area of an infiltration basin.
- The arrival time of recharge from a drywell is shorter than an infiltration basin.
- Five drywells can infiltrate and recharge more water than a 70 m diameter infiltration basin.
- The benefit of a drywell still holds after 20 years of steady-state operation.
- Low permeability subsurface layers can be bypassed using a drywell and infiltration basin combination.

Chapter 7
- The overall daily water input data shows the filling up sedimentation chamber (SC1), drywell (DW1), SC2, and DW2 and subsequent draining in a consistent pattern.
- The SC1 and DW1 is directly connected, and water from SC1 leaks through the sidewall to the DW1, and similar behavior is observed for SC2 and DW2.
- The old drywell and new drywell are connected only through the connection pipe and act as a MaxWell Plus system.
- No significant reduction in hydraulic performance of DW1 and DW2 was observed since 2019.
- Turbidity data shows that both SC1 and SC2 received a significant amount of clay during daily inflow and rain events.
- Sediments in SCs escape through the overflow pipe into the lower chambers.

- The perched water table responds to the rain events, but no significant responses were observed on daily inflow.
- The infiltration rate of the perched water table is extremely low.
- The water content sensors below the perched layer show no movement of water
- Groundwater level shows daily pumping events.
- Groundwater level shows annual decline during excessive pumping in summer, and the water level rises back to the pre-winter value in winter months
- The daily change in groundwater level due to pumping activity hinders the accurate estimation of the recharge rate from MAR.

9. REFERENCE

Akan, A.O., 2002. Modified rational method for sizing infiltration structures. Canadian Journal of Civil Engineering, 29(4): 539-542.

Ammann, A.A., Hoehn, E., Koch, S., 2003. Ground water pollution by roof runoff infiltration evidenced with multi-tracer experiments. Water Research, 37(5): 1143-1153.

Bandeen, R.F., 1984. Case study simulations of dry well drainage in the tucson basin, College of Engineering University of Arizona Tucson, Arizona 85721, Water Resources Research Center.

Bandeen, R.F., 1987. Additional case study simulations of dry well drainage in the tucson basin, The University of Arizona Campus Repository, Water Resources Research Center. DOI:http://hdl.handle.net/10150/306945

Bouwer, H., 2002. Artificial recharge of groundwater: Hydrogeology and engineering. Hydrogeology journal, 10(1): 121-142. DOI:10.1007/s10040-001-0182-4

Bradford, S.A., Torkzaban, S., 2015. Determining parameters and mechanisms of colloid retention and release in porous media. Langmuir, 31(44): 12096-105. DOI:https://doi.org/10.1021/acs.langmuir.5b03080

Cadmus, 1991. Storm water drainage wells (5d2), Waltham, MA.

Cadmus, 1996. Storm water drainage well guidance - draft, Waltham, MA.

Cadmus, 1999. State-by-state notebooks compiling results from the class v underground injection control study, United States Environmental Protection Agency.

Chappelle, C., Hanak, E., Harter, T., 2017. Groundwater in california, Public Policy Institute of California.

City of Portland, O., 2015. Underground injection control management plan, City of Portland, Bureau of Environmental Services.

Dechesne, M., Barraud, S., Bardin, J.-P., 2004. Spatial distribution of pollution in an urban stormwater infiltration basin. J Contam Hydrol, 72(1-4): 189-205.

Dechesne, M., Barraud, S., Bardin, J.-P., 2005. Experimental assessment of stormwater infiltration basin evolution. Journal of Environmental Engineering, 131(7): 1090-1098.

Dechesne, M., Barraud, S., Bardin, J.-P., Alfakih, E., 2001. Long-term performance of stormwater infiltration basins, Bridging the Gap: Meeting the World's Water and Environmental Resources Challenges, pp. 1-8.

Dettinger, M., 2011. Climate change, atmospheric rivers, and floods in california – a multimodel analysis of storm frequency and magnitude changes1. JAWRA Journal of the American Water Resources Association, 47(3): 514-523. DOI:10.1111/j.1752-1688.2011.00546.x

Dillon, P., Pavelic, P., Sibenbaler, X., Gerges, N., Clark, R., 1999. Development of new water resources by aquifer storage and recovery using stormwater runoff. International Water and Irrigation, 19(2).

Dillon, P., Toze, S., Page, D., Vanderzalm, J., Bekele, E., Sidhu, J., Rinck-Pfeiffer, S., 2010. Managed aquifer recharge: Rediscovering nature as a leading edge technology. Water Science and Technology, 62(10): 2338-2345. DOI:10.2166/wst.2010.444

Edwards, E.C., 2017. Assessing the groundwater contamination risk of drywell-induced stormwater infiltration using analytical and numerical methods. University of California, Davis.

EPA, 1999. The class v underground injection control study, United States Environmental Protection Agency, Office of Ground Water Drinking Water.

Faunt, C.C., Sneed, M., Traum, J., Brandt, J.T., 2016. Water availability and land subsidence in the central valley, california, USA. Hydrogeology journal, 24(3): 675-684.

Feighery, J., Mailloux, B.J., Ferguson, A.S., Ahmed, K.M., van Geen, A., Culligan, P.J., 2013. Transport of e. Coli in aquifer sediments of bangladesh: Implications for widespread microbial contamination of groundwater. Water Resources Research, 49(7): 3897-3911. DOI:10.1002/wrcr.20289

Ferguson, B.K., 1994. Stormwater infiltration. CRC Press.

Ghasemizade, M., Asante, K.O., Petersen, C., Kocis, T., Dahlke, H.E., Harter, T., 2019. An integrated approach toward sustainability via groundwater banking in the southern central valley, california. Water Resources Research, 55(4): 2742-2759.

Gray, D.M., Norum, D., 1967. The effect of soil moisture on infiltration as related to runoff and recharge, Proceedings of hydrology symposium. Citeseer.

Gunnarsdottir, M., Gardarsson, S., Andradottir, H., 2013. Microbial contamination in groundwater supply in a cold climate and coarse soil: Case study of norovirus outbreak at lake mývatn, iceland. Hydrology Research, 44(6): 1114-1128.

Hanak, E., Lund, J.R., 2012. Adapting california’s water management to climate change. Climatic Change, 111(1): 17-44. DOI:10.1007/s10584-011-0241-3

Harter, T., 2015. California's agricultural regions gear up to actively manage groundwater use and protection. California Agriculture, 69(3): 193-201.

Heberger, M., Cooley, H., Herrera, P., Gleick, P.H., Moore, E., 2011. Potential impacts of increased coastal flooding in california due to sea-level rise. Climatic Change, 109(1): 229-249. DOI:10.1007/s10584-011-0308-1

Howitt, R., Medellín-Azuara, J., MacEwan, D., Lund, J.R., Sumner, D., 2014. Economic analysis of the 2014 drought for california agriculture. Center for Watershed Sciences University of California, Davis, CA.

Izuka, S.K., 2011. Potential effects of roadside dry wells on groundwater quality on the island of hawaii-assessment using numerical groundwater models, U.S. Geological Survey.

Jurgens, B.C., Burow, K.R., Dalgish, B.A., Shelton, J.L., 2008. Hydrogeology, water chemistry, and factors affecting the transport of contaminants in the zone of contribution of a public-supply well in modesto, eastern san joaquin valley, california, U. S. Geological Survey.

Kazemi, F., Golzarian, M.R., Myers, B., 2018. Potential of combined water sensitive urban design systems for salinity treatment in urban environments. Journal of Environmental Management, 209: 169-175.

Kennedy, J., Goodrich, D., Unkrich, C., 2013a. Model enhancements for urban runoff predictions in the south-west united states 2182. Predictions in Ungauged Basins. Cambridge University Press, pp. 332-337.

Kennedy, J.R., Goodrich, D.C., Unkrich, C.L., 2013b. Using the kineros2 modeling framework to evaluate the increase in storm runoff from residential development in a semiarid environment. Journal of Hydrologic Engineering, 18(6): 698-706.

Kerr, R.A., 2001. Rising global temperature, rising uncertainty. Science, 292(5515): 192. DOI:10.1126/science.292.5515.192

Kocis, T.N., Dahlke, H.E., 2017. Availability of high-magnitude streamflow for groundwater banking in the central valley, california. Environmental Research Letters, 12(8): 084009.

Lal, R., Logan, T., 1995. Agricultural activities and greenhouse gas emissions from soils of the tropics. Soil management and greenhouse effect: 293-307.

Mantoglou, A., Gelhar, L.W., 1987. Effective hydraulic conductivities of transient unsaturated flow in stratified soils. Water Resources Research, 23(1): 57-67.

Mays, D.C., Hunt, J.R., 2005. Hydrodynamic aspects of particle clogging in porous media. Environmental science & technology, 39(2): 577-584.

Milczarek, M., J. Banuelos, Rice., R., 2020. Fort irwin test well and monitor well installation report, U.S. Environmental Protection Agency, Washington, DC. DOI:https://cfpub.epa.gov/si/

Montz, B., 2000. The generation of flood hazards and disasters by urban development of floodplains. Floods, 1: 116-127.

Mote, P.W., Li, S., Lettenmaier, D.P., Xiao, M., Engel, R., 2018. Dramatic declines in snowpack in the western us. Npj Climate and Atmospheric Science, 1(1): 1-6.

Newcomer, M.E., Gurdak, J.J., Sklar, L.S., Nanus, L., 2014. Urban recharge beneath low impact development and effects of climate variability and change. Water Resources Research, 50(2): 1716-1734.

Niswonger, R.G., Morway, E.D., Triana, E., Huntington, J.L., 2017. Managed aquifer recharge through off-season irrigation in agricultural regions. Water Resources Research, 53(8): 6970-6992.

Pavelic, P., Dillon, P., Robinson, N., 2005. Modelling of well-field design and operation for an aquifer storage transfer and recovery (astr) trial, Pro IAH XXXI Congress:" New Approaches to Charactering Groundwater Flow. Swets Zeitlinger Lisse, pp. 859-862.

Rizwan, T., Bhattacharjee, S., 2009. Particle deposition onto charge-heterogeneous substrates. Langmuir, 25(9): 4907-4918.

Rodell, M., Famiglietti, J.S., Wiese, D.N., Reager, J., Beaudoing, H.K., Landerer, F.W., Lo, M.-H., 2018. Emerging trends in global freshwater availability. Nature, 557(7707): 651-659.

Sasidharan, S., Bradford, S.A., Simunek, J., De Jong, B., S, R.K., 2018. Evaluating drywells for stormwater management and enhanced aquifer recharge. Adv Water Resour, 116: 167-177. DOI:10.1016/j.advwatres.2018.04.003

Sasidharan, S., Bradford, S.A., Simunek, J., Kraemer, S.R., 2019. Drywell infiltration and hydraulic properties in heterogeneous soil profiles. J Hydrol (Amst), 570: 598-611. DOI:10.1016/j.jhydrol.2018.12.073

Sasidharan, S., Bradford, S.A., Šimůnek, J., Kraemer, S.R., 2020. Groundwater recharge from drywells under constant head conditions. Journal of Hydrology, 583: 124569. DOI:10.1016/j.jhydrol.2020.124569

Sasidharan, S., Bradford, S.A., Šimůnek, J., Kraemer, S.R., 2021. Virus transport from drywells under constant head conditions: A modeling study. Water Research, 197: 117040. DOI:https://doi.org/10.1016/j.watres.2021.117040

Scherberg, J., Baker, T., Selker, J.S., Henry, R., 2014. Design of managed aquifer recharge for agricultural and ecological water supply assessed through numerical modeling. Water Resources Management, 28(14): 4971-4984.

Schilling, O.S., Irvine, D.J., Hendricks Franssen, H.J., Brunner, P., 2017. Estimating the spatial extent of unsaturated zones in heterogeneous river-aquifer systems. Water Resources Research, 53(12): 10583-10602.

Schwalm, C.R., Williams, C.A., Schaefer, K., Baldocchi, D., Black, T.A., Goldstein, A.H., Law, B.E., Oechel, W.C., Scott, R.L., 2012. Reduction in carbon uptake during turn of the century drought in western north america. Nature Geoscience, 5(8): 551-556.

Šimůnek, J., van Genuchten, M.T., 2008. Modeling nonequilibrium flow and transport processes using hydrus. Vadose Zone Journal, 7(2): 782-797.

Šimůnek, J., van Genuchten, M.T., Šejna, M., 2016. Recent developments and applications of the hydrus computer software packages. Vadose Zone Journal, 15(7): 25. DOI:10.2136/vzj2016.04.0033

Snyder, D.T., Morgan, D.S., McGrath, T.S., 1994. Estimation of ground-water recharge from precipitation, runoff into drywells, and on-site waste-disposal systems in the portland basin, oregon and washington, US Geological Survey; Earth Science Information Center, Open-File Reports Section [distributor].

Sprenger, C., Hartog, N., Hernández, M., Vilanova, E., Grützmacher, G., Scheibler, F., Hannappel, S., 2017. Inventory of managed aquifer recharge sites in europe: Historical development, current situation and perspectives. Hydrogeology journal, 25(6): 1909-1922.

Teatini, P., Comerlati, A., Carvalho, T., Gütz, A.-Z., Affatato, A., Baradello, L., Accaino, F., Nieto, D., Martelli, G., Granati, G., 2015. Artificial recharge of the phreatic aquifer in the upper friuli plain, italy, by a large infiltration basin. Environmental Earth Sciences, 73(6): 2579-2593.

Torkzaban, S., Bradford, S.A., Vanderzalm, J.L., Patterson, B.M., Harris, B., Prommer, H., 2015. Colloid release and clogging in porous media: Effects of solution ionic strength and flow velocity. J Contam Hydrol(0). DOI:http://dx.doi.org/10.1016/j.jconhyd.2015.06.005

U.S.EPA, 2021. Enhanced aquifer recharge of stormwater in the united states: State of the science review. , Environmental Protection Agency, Office of Research and Development, Washington, DC; EPA/600/R-21/037F. .

Wamsley, L., 2017. Mother of all landslides' in big sur buries section of california's highway 1, NPR.
Washington State Department of Ecology, 2006. Guidance for uic wells that manage stormwater, Washington State Department of Ecology Water Quality Program.
Williams, A.P., Allen, C.D., Macalady, A.K., Griffin, D., Woodhouse, C.A., Meko, D.M., Swetnam, T.W., Rauscher, S.A., Seager, R., Grissino-Mayer, H.D., 2013. Temperature as a potent driver of regional forest drought stress and tree mortality. Nature Climate Change, 3(3): 292-297.
Williams, A.P., Cook, E.R., Smerdon, J.E., Cook, B.I., Abatzoglou, J.T., Bolles, K., Baek, S.H., Badger, A.M., Livneh, B., 2020. Large contribution from anthropogenic warming to an emerging north american megadrought. Science, 368(6488): 314-318.
Wilson, L.G., Osborn, M.D., Olson, K.L., Maida, S.M., Katz, L.T., 1990. The ground-water recharge and pollution potential of dry wells in pima county, arizona. Ground Water Monitoring and Remediation, 10(3): 114-121. DOI:DOI 10.1111/j.1745-6592.1990.tb00010.x
Wright, P., 2019. California's big sur's $54 million 'catastrophic landslide' a result of drought followed by deluge, scientists say, weather.com. The Weather Company’s.
Xiao, M., Udall, B., Lettenmaier, D.P., 2018. On the causes of declining colorado river streamflows. Water Resources Research, 54(9): 6739-6756.
Xie, Y., Cook, P.G., Brunner, P., Irvine, D.J., Simmons, C.T., 2014. When can inverted water tables occur beneath streams? Groundwater, 52(5): 769-774.
Yeh, T.C.J., Gelhar, L.W., Gutjahr, A.L., 1985a. Stochastic analysis of unsaturated flow in heterogeneous soils: 1. Statistically isotropic media. Water Resources Research, 21(4): 447-456.
Yeh, T.C.J., Gelhar, L.W., Gutjahr, A.L., 1985b. Stochastic analysis of unsaturated flow in heterogeneous soils: 3. Observations and applications. Water Resources Research, 21(4): 465-471. DOI:10.1029/WR021i004p00465